NONLINEAR FINITE ELEMENT SIMULATION OF THE TEST PROCEDURE FOR STIFFENED PANELS UNDER COMBINED LATERAL AND IN-PLANE LOADS

by

Thomas S. Z. Hu

DTIC QUALITY INSPECTED 4

Defence

Research

Establishment

Atlantic

Centre

Recherches pour la

Défense

Atlantique

Canada

19970911 076

National Defence
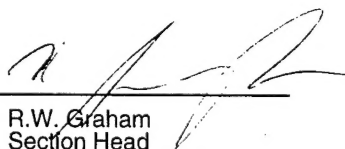Research and
Development Branch

Défense nationale
Bureau de recherche
et développement

NONLINEAR FINITE ELEMENT SIMULATION OF THE TEST PROCEDURE FOR STIFFENED PANELS UNDER COMBINED LATERAL AND IN-PLANE LOADS

Thomas S. Z. Hu

November 1996

Approved by: R.W. Graham
Section Head
Hydronautics Section

TECHNICAL MEMORANDUM 97/ 219

**Defence
Research
Establishment
Atlantic**

**Centre de
Recherches pour la
Défense
Atlantique**

Canada

Abstract

DREA conducted a joint structural testing project with the U.S. Interagency Ship Structures Committee (SSC) at C-FER (Centre For Engineering Research Inc., Edmonton) earlier this year. Twelve stiffened plates, seven without damage and five with damage, having dimensions approximately equal to a typical stiffened panel at the strength deck of the Canadian Patrol Frigate (CPF) were tested. One of the objectives of this project was to conduct a computer simulation of the test procedure with the non-linear finite element method. It was hoped that after a successful simulation, panels with other dimensions and parameters could be studied numerically. As the scientific authority of this project, the author planned the test procedure, conducted the numerical prediction of the collapse load of the specimens, and performed the computer simulation of the test procedure. Because of the complexity of the computer simulation and completely different behaviour between damaged and undamaged specimens, this memorandum only summarises the finite element results on specimens without damage and their relation with the test observations. Seven specimens, which failed either in tripping or in combined plate and flexural buckling modes under combined lateral and axial loads, were modelled. Some interesting buckling phenomena were discovered and are discussed.

Résumé

Au début de l'année, le CRDA a entrepris un project d'essais de structures avec l'Interagency Ship Structures Committee (SSC) américain au C-FER (Center for Engineering Research Inc., à Edmonton). Les essais ont porté sur douze plaques raidies, sept intactes et cinq endommagées, de dimensions à peu près égales à celles d'un panneau raidi typique du pont de résistance de la Frégate canadienne de patrouille (FCP). L'un des objectifs de ce project était d'effectuer une simulation sur ordinateur de la procédure d'essai au moyen de la méthode par éléments finis non linéaires. On espérait qu'après une deuxième simulation réussie, on serait en mesure d'étudier numériquement des panneaux de dimensions et paramètres différents. En tant que responsable scientifique de ce project, l'auteur a planifié la méthode d'essai, effectué la prédiction numérique de la charge de défaillance des éprouvettes, et réalisé la simulation informatique de la méthode d'essai. À cause de la complexité de la simulation informatique et du comportement complètement différent des éprouvettes intactes et des éprouvettes endommagées, cette note se contente de résumer les résultats des éléments finis sur les éprouvettes intactes et leur relation avec les observations de l'essai. On a modélisé sept éprouvettes qui ont flambé en torsion ou dont les plaques et raidisseurs ensemble ont flambé en flexion sous des charges latérales et axiales combinées. Certains phénomènes intéressants de flambement qui ont été découverts font l'objet d'une discussion.

DREA TM/97/219
Non-linear Finite Element Simulation of the Test Procedure for Stiffened Panels under Combined Lateral and In-plane Loads
by
Thomas S.Z. Hu

Executive Summary

Introduction
Buckling of stiffened plates is one of the most important considerations in ship structural design. DREA conducted a joint test project with the U.S. Interagency Ship Structural Committee (SSC) earlier this year. A total of twelve stiffened panels, with or without damage, having dimensions approximately equal to a typical stiffened panel at the strength deck of the Canadian Patrol Frigate (CPF), were tested at C-FER (Centre For Engineering Research Inc., Edmonton). DREA lead this project on behalf of SSC and conducted the non-linear finite element analysis to predict the response and the collapse load of the specimens. Because of the complexity of the numerical simulation and the completely different behaviour between damaged and undamaged specimens, this memorandum summarises the finite element results of the first seven specimens - those without damage under combined lateral and in-plane loads.

Principal Results
One of the main objectives of this project was to establish a test frame capable of testing a single stiffened panel under in-plane and lateral loads. This frame could also be used to study the behaviour of damaged and corroded panels. Another objective was to perform a computer simulation of the test procedure so that panels with other dimensions and parameters could be analysed with the non-linear finite element method. Test specimens failed either in tripping or in a combined plate and flexural buckling mode. The finite element results showed good agreement with the test observation for both load-shortening curves and buckling shapes. Interesting phenomena regarding the influence of lateral load on tripping behaviour were also discovered and were discussed.

Significance of Results
This project provided important information for improving the buckling and tripping criteria in current design standards. It also gave experimental verification of the simplified numerical models used in predicting the overall hull collapse. The finite element method was found capable of simulating the test procedure.

Future Plans
Because of the successful simulation of the test procedure, panels with other configurations and parameters can be modelled and studied in future. The second series of tests with specimens with deliberate damage or dents is being analysed. Other types of failure modes such as grillage and overall hull collapse will also be investigated in the future.

Contents

List of Figures

List of Tables

Nomenclature:

bf, bp	flange width, plate width
dw	web height
R_x, R_y, R_z	rotation about X, Y or Z axis
tf, tp, tw	flange thickness, plate thickness, web thickness
U_x, U_y, U_z	displacement in X, Y or Z axis

1. Introduction

Ships experience hogging and sagging deformations under wave loading. In addition to the hydrostatic pressure, the stiffened panels that form the ship hull undergo repeated compressive and tensile forces. The compressive strengths of these panels are normally less than their tensile strength. In other words, the buckling modes are always the dominant failure modes. Besides local plate buckling, ship hulls can buckle in several different modes. These modes include the buckling of an individual stiffened panel either in the flexural buckling mode or in the tripping mode, the grillage buckling, and the ultimate hull collapse. In some cases, the buckling modes are interconnected and can occur simultaneously or happen one after another.

Fabrication of such stiffened panels requires the plates to be fully welded to the stiffeners. The fabrication process generates unavoidable imperfections including geometric imperfections and residual stresses in plates and stiffeners. Depending on the magnitudes, the imperfections can significantly change the buckling strength of the panels, especially in the elastic-plastic region. The design criteria cannot not be established without considering these.

The flexural buckling strength of the stiffened panel is one of the major considerations in ship structural design. It is used to determine the dimensions of the plates and the stiffeners. After the size of the components are chosen, the designers evaluate other buckling criteria to ensure that buckling modes of other types will not occur. For example, a stiffened panel needs to be checked against tripping criteria to ensure the stiffener has sufficient lateral support. Currently, the tripping criteria are based on formulas derived from elastic theory with large safety factors [1]. These criteria may not be appropriate [2] as the design philosophy is shifting from the working stress design to the load resistance factor design [3].

The overall ultimate collapse of the ship hull has become a design criterion in the latest design standard [1]. To evaluate the overall ultimate hull collapse moment [4,5] requires information on the load-shortening curve of the individual stiffened panel. This information can be obtained through numerical methods. It is, however, difficult in numerical models to take the effects of the residual stresses and imperfections into consideration.

During operation, ships may suffer various damage such as corrosion from the environment or dents from external forces. In order to make efficient repair decisions, one needs to assess the residual strength of the damaged panels. The assessment can be carried out with numerical models but this requires experimental confirmation.

In considering the importance of the buckling strength information in ship structural design, DREA proposed a test project to the U.S. Interagency Ship Structures Committee (SSC). This proposal was accepted by the SSC. To increase the scope of the project, SSC

and DREA agreed to fund the work jointly and DREA lead the contract on behalf of SSC.

One of the objectives of this test was to establish a test frame capable of testing an in-plane and laterally loaded stiffened plate. Special boundary and loading conditions were needed to represent the structural behaviour of a stiffened panel in a grillage environment. The other objective was to conduct the computer simulation of the test procedure and to predict the response of the specimens with the non-linear finite element method. It was hoped that after a successful simulation, panels with other dimensions under various loading combinations and damage could be modelled numerically.

This project was contracted out to an Edmonton based company C-FER. DREA agreed to plan the test procedure and to conduct the non-linear finite element simulation. Twelve stiffened panels with dimensions similar to those on the strength deck of CPF were tested. These specimens were either under combined in-plane and lateral loads or had deliberate damage and in-plane loading.

Because of the complexity of the numerical simulation and completely different behaviour between damaged and undamaged specimens, this memorandum only reports the results of the first seven specimens (combined in-plane and lateral loads). The test procedures including the imperfection and residual strain measurements, the test frame set-up and the load applications are summarised in Section 2. Non-linear finite element analyses are performed using the commercial finite element program ADINA [6]. The numerical models including the detail of the mesh division, boundary conditions and the modelling techniques of the residual stress and geometric imperfections are described in Section 3. The comparisons of the finite element results with the test observations and discussion of the results are reported in Section 4.

2. Test Procedure

To avoid the confusion of the mixed buckling modes involving individual stiffened panel buckling and grillage collapse, the test set-up was intentionally designed for single stiffened plate testing. The specimens represented a single stiffened panel cut out of a grillage between transverse frames. It was assumed to be simply supported at both ends with symmetric boundary conditions along the sides. The following information about the specimens and the description of the test set-up are required for the finite element modelling.

2.1 Specimen geometry

The geometry of the stiffened panel was similar to that used on the strength deck of CPF. Based on the measurement of all specimens, the mean values of the dimension were $b_p \times t_p = 500.4$ mm $\times$ 9.67 mm; $b_f \times t_f = 103.9$ mm $\times$ 8.06 mm; and $d_w \times t_w = 136.8$ mm $\times$ 6.22 mm. The length of the specimen was 2000 mm. These values were used in the finite element geometric definitions.

2.2 Material properties

The stiffener was hot-rolled grade 350 WT tee section (127 mm $\times$ 102 mm) and the plate was made of hot-rolled 350WT steel. Tension coupons (cut from the plates, webs and flanges of the stiffeners), were tested to determine the material properties. The stress-strain curves of these coupons showed a noticeable yield plateau of a typical hot-rolled structural steel. The static yield stresses of different components of the stiffened panels were 425 MPa for the plate, 411 MPa for the web, and 395 MPa for the flange.

2.3 Residual stresses

The plate was cut by hydraulic jets to minimise the zone affected by local plastic deformation at the edges. A twin-head sub-arc weld process was used for the 6 mm fillet weld between the stiffener and the plate. Longitudinal residual strains were measured using a sectioning method with mechanical strain gauges (100 mm gauge length). A total of 75 strips were cut from a 300 mm long segment. The procedure assumed that the longitudinal strains were uniformly distributed across the thickness and length. The measurements resulted in a residual stress pattern similar to that in a typical welded steel component which has a narrow tensile yield zone close to the weld which sharply drops to compression at a short distance from the weld.

2.4 Initial imperfections

The initial imperfections of the test specimens were measured before testing. The procedure employed a Nardini-SZ25120T lathe machine to provide a three-dimensional reference system as shown in **Figure 1**. Displacement gauges mounted on the carriage of

3

the lathe machine travelled along the surfaces of the specimen to collect profile data at specified locations. There were in total 19 data points along the length of the panel and 5 lines across the panel including the junction of the web and the plate. The same number of data points were also measured along the length of the junction of the web and flange, and along both edges of the flange. The imperfection data was referred to an orthogonal Cartesian co-ordinate with the panel located on the x-y plane. The origin of the plate was located at the mid-span of the junction of the plate and the web with the z-axis toward the toe of the Tee as shown in **Figure 2**.

2.5 Test set-up

Experimental simulation of the symmetric boundary conditions was the most difficult part of the test set-up. It was physically impossible to build a continuously symmetric boundary. The symmetric boundary could only be achieved at discrete locations. The question was how many discrete locations were required to approximate the continuous boundary condition. Another consideration was the mechanical restriction. Only a limited number of discrete boundary devices could be mounted along the fixed length of the edges.

The original design of the test set-up is shown in **Figure 3**. C-FER found other mechanical parts that were easier to assemble and had less friction. The schematic plot of the final design is shown in **Figure 4**. It was composed of several main carriages on each side of the panel. Each carriage, with an inner linear bearing, travelled along two main rails. The two main rails in turn were mounted on the supported frames. Each carriage contained a secondary carriage. This secondary carriage, with the same bearing system, travelled orthogonally on top of the main carriage. A grip fixture mounted on a rotational bearing was located at the centre of the secondary carriage. It allowed the edge of the plate to rotate normally to the carriage. The specimen was positioned vertically under the Tubular Testing System (TTS) at C-FER laboratory as shown in **Figure 5**. The cylindrical bearing at both ends provided simple supports and transferred the reactions of the lateral load through friction. Hydraulic jacks attached to the wall applied the lateral load at two third points through two 100 kN rams while the axial load was applied from the TTS head.

The symmetric boundary allowed the edge of the plate to rotate about the y-axis and to move in the x and z directions. A preliminary finite element study had shown that the more discrete grip points the better. However, in considering the size of the carriages and the cost, it was decided to use five carriages on each side of the panel. **Figure 6** shows the cross sectional view of the test set-up.

2.6 Load application

A small initial axial load was applied on the specimen to generate enough friction force between the cylinder and the end plates to keep the specimen in place. This initial axial load was a small portion of the expected peak load and the plate remained elastic at this

4

stage. The lateral load was then applied and remained constant through the whole test. Since the load-shortening response of the specimen was expected to have a linear elastic portion which gradually turned into the peak load followed by a descending branch, a load control method was used for the axial load before the peak load. It changed to displacement control when the response passed the elastic limit.

3. Finite Element Model

Since the specimens were expected to experience large displacements and plastic deformation, a finite element study was required to model both geometric and material non-linearities. The commercial software ADINA which enabled modelling of geometric and material non-linearities was chosen in this study.

3.1 General

A four-node quadrilateral shell element, from the family of the degenerate iso-parametric shell elements, with a $2 \times 2 \times 2$ integration order was used to model the plate and the stiffener. The kinematic assumption that was made was large displacement and rotation but small strain. Since the coupon tests had shown a clear plateau, the material modelling of the plate was assumed to be bilinear elastic-perfectly-plastic with a von Mises yield condition. In order to obtain the entire load-shortening curve, the automatic displacement control method was used in the solution scheme. The lateral load was applied through load control.

3.2 Imperfections

The imperfections of the finite element model were directly mapped from the test measurements. Since there was no measurement along the edges of the plate, linear extrapolation was used to obtain the edge profiles. After the mesh size was decided, linear interpolation was then used to obtain the finite element nodal points. **Figure 7** shows the mapping process from the original measurement to the finite element mesh. In order to compare the geometry in the mapping process visually, these imperfections are enlarged 15 times.

3.3 Finite element mesh

Previous convergence studies indicated a mesh size of 16×24 was sufficient to catch the buckling behaviour. However, the purpose of this analysis was to simulate the behaviour of the test specimen. In considering the boundary supports and the residual stress pattern, a finer mesh was used so that the nodal points would coincide with the boundary gripping devices. The final mesh sizes were 16×38 for the plate; 6×38 for the web; and 4×38 for the flange.

The co-ordinate system for the finite element model was the same as for the test measurement as shown in **Figure 8**. It refers to an orthogonal Cartesian co-ordinate system with the mid-plane of the plate located in the x-y plane. The origin was located at the mid-span of the model at the junction of the web with the plate parallel to the x-axis. The positive z-axis was toward the junction of the toe of the stiffener. The mesh was designed so that each grip fixture contained two elements.

6

3.4 Boundary conditions

The grip fixture was physically restrained against translation in the y-direction and against rotation in the x- and z- directions. Two types of modelling options were used. The first model designated the central node of the grip fixture to be the master node. The other two points at the same grip fixture were rigidly linked to the master node. The second model replaced the rigid link with two thicker elements on top of the plate as shown in **Figure 8**. Preliminary results indicated both models gave a similar response. Model 2 was used in all the analyses thereafter.

The ends of the specimen had thick end plates. The purpose of these plates was to ensure that the ends remained plane during deformation. The thick plates were not modelled physically but "the plane sections remain plane" condition was achieved by assigning the end nodes to be slave nodes so they could displace together with respect to a master node. As indicated in **Figure 6**, the specimen was mounted between two cylindrical heads. There was a distance (38.1 mm) between the centre of the half-cylinder and the end of the specimen. When the plate started to buckle, a slight eccentricity developed. To account for this eccentricity, the master node was offset 38.1 mm from the end of the plate.

3.5 Residual stresses

One of the focal points of the investigation was to measure the magnitude and distribution of residual stresses and their effects. The residual stresses in a stiffened panel came from two sources; one from the welding of the stiffener to the plate and the other from the manufacturing process to position the components in the right locations. One common assumption is that the residual stress pattern forms rectangular tensile and compressive stress blocks in the transverse direction and is constant in longitudinal direction. However, the residual stress in a real panel is in a tri-axial state and varies not only in the transverse direction but also parallel to the weld. It was decided to introduce the residual stress in the panel in a way that resembles the actual welding procedure. The residual stresses thus were generated through temperature variations on nodal points adjacent to the weld. The magnitude of the residual stress could be calibrated by changing the temperature magnitude or by varying the coefficient of thermal expansion.

3.6 Residual stresses and imperfection modelling

The introduction of thermal residual stress caused additional deformation and changed the nodal co-ordinates such that they were inconsistent with the input geometric imperfections, since the geometry after welding (i.e. introducing residual stress) should have been used as the initial geometry. To avoid the change of the initial imperfection, the procedure described in References [7] and [8] was used. This procedure has been successfully applied and verified in fabricated tubular structures used in offshore oil platforms. **Figure 9** shows the procedure used for the automatic generation of welding residual stresses with retention

7

of the initial imperfections and is explained as follows:

Step 1. Create imperfections through the mapping process and generate the finite element mesh while the nodes adjacent to the weld have positive temperature loading.

Step 2. Activate the temperature loading and produce reversed residual stresses. The panel is strained in the opposite sense to the final residual stress distribution. The updated nodal geometry is stored in a file.

Step 3. Read this geometry file as the original geometry; therefore the imperfections in the model include geometric imperfections and deformation due to positive temperature variations. The plate is free of residual stresses. The nodes adjacent to the weld have negative temperature loading.

Step 4. Activate the temperature loading at the first loading step. This results in a panel with the desired residual stresses and imperfections approximating the initial imperfections. The imperfections can be verified by comparing the nodal co-ordinates of the panel at the end of this step with step 1.

3.7 Time functions

Non-linear collapse analysis was done by applying loads or displacements in small load steps. An iteration procedure was then used to achieve convergence. The finite element modelling of the test procedure involved four time functions. A total of fifty time steps were applied on the models. The time functions as shown in **Figure 10** are described as follows:

The temperature load is applied as a step function and kept constant throughout the analysis. The lateral load is started at time step 4, increased to step 5 and kept constant through the analysis. The bending moments generated by the lateral load are also kept constant through the analysis. The axial displacement loading is applied linearly from step 5 to step 50.

4. Numerical Results

Seven panels have been analysed and compared with the test results. Five of them had the gripping devices mounted at the sides while the other two had the boundary gripping devices removed to verify the effectiveness of the devices. The load combinations, boundary conditions and the lateral load direction of the specimens as well as the results are listed in **Table 1**. The effect of the residual stress and the structural response are explained in this section.

Table 1: Summary of the finite element and test results

Specimen No.	Lateral load	B.C. at sides	Peak load (kN)		Ratio (FEA/Test)	Test failure mode	FEA failure mode
			Test	FEA			
1.3	25 kN	yes	1453	1489	1.025	flexural	flexural
1.1	10 kN	yes	1572	1635	1.040	flexural	flexural
1.2	0 kN	yes	1736	1759	1.013	flexural	flexural
1.6†	-10 kN	yes	1673	1868	1.117	tripping	flexural
1.6‡	-15 kN	yes	1673	1454	0.869	tripping	tripping
1.4	-25 kN	yes	1275	1285	1.008	tripping	tripping
1.7	25 kN	no	1361	1436	1.055	flexural	flexural
1.5	-25 kN	no	1139	1208	1.061	tripping	trippimg

- lateral load is applied at two-third points
- lateral load is applied at junction of plate and web
- negative lateral load is from flange toward plate so that plate is in tension initially
- positive lateral load is from plate toward flange so that plate is in compression initially
- † There are large discrepancies in both the peak load and the buckling mode between the finite element analysis and the test results.
- ‡ The lateral load in the finite element is increased to 15 kN instead of 10 kN. The additional 5kN load has changed the buckling mode as well as peak load completely.

4.1 Effect of the residual stress

Both the residual stress pattern and their magnitude are required to be similar to the test measurements. The deformations due to temperature variation should be small so that the panel has as little plastic deformation as possible. On the other hand, the magnitude of the temperature loading should be sufficiently high so that enough residual stress can be generated. It was hoped that after the temperature variation in step 4, the panel would be

9

able to shrink back to its original shape but with the desired residual stress pattern and level. Models with residual stresses could be verified by comparing the nodal geometry in step 4 with that in step 1 to verify its imperfection profile. This was a trial and error process.

Various levels of temperature variation were applied at both the junctions of the plate and web; and the flange and web. It was found that a temperature variation of 200°C at the junction of the plate and web and 50°C at the junction of the web and flange was an acceptable combination. Under this temperature variation, enough residual stress was generated and the initial imperfections of the plate were maintained. The maximum difference in the nodal geometry after the temperature variation was less than 10^{-2} mm. To further investigate the effects of these differences, models with nodal geometry of step 4 with residual stress removed were re-run and compared with those having the nodal geometry of step 1. The results showed that there were no differences in both the load displacement response and the buckling shape.

After activating the negative nodal temperature, a residual stress pattern with tensile stress close to the yield stress of the material was created. The comparison of the finite element results to the test measurements is shown in **Figure 11**. The finite element results represent the stress at the nearest integration points of elements at the mid-span. Since the residual stress measurements were only a rough estimation, this residual stress pattern was considered to be a reasonable approximation. The load-shortening curves for the finite element model of specimen 1.2 with and without residual stresses are shown in **Figure 12**. The peak load drops from 1920 kN for the model without residual stress to 1759 kN for the model with residual stress.

4.2 Expected deformed shape

In the test, the specimens were placed under the loading head in such a way that the axial load went through the neutral axis (calculated with full plate width) of the specimens. Because of symmetry, the weakest principal axis coincided with the web of the stiffener. As a result of the buckling, the overall panel can deform in two ways; one is deflection toward the flange (higher compressive stresses in plate) and the other is deflection toward the plate (higher compressive stresses in flange). Using the same terminology as in Reference 8, the former is called plate-induced failure mode (flexural buckling) and the latter is called the stiffener-induced failure mode. If the panel fails in a stiffener-induced failure mode and the flange does not have sufficient lateral support, the stiffener will twist as it bends. This type of mode is called tripping. Besides the overall panel buckling, the plate may buckle between the stiffener and gripping devices. The local buckling of the stiffener, however, was excluded from the failure mode because of the low width to thickness ratio of the specimens.

The buckling of the plate depends on its physical properties and the boundary conditions. As an example, if the plate is simply supported around four edges, the buckling shape

associated with the smallest buckling load is a single half-wave in the transverse direction and several half-waves in the longitudinal direction. Furthermore, the plate will develop an alternate pattern on both sides of the stiffener. If the plate buckling load is lower than the overall panel buckling load, i.e. the plate buckling always occurs prior to the overall panel buckling, the overall panel buckling will exhibit a mixed mode.

The effective width concept states that the buckling of the plate will decrease the width of the plate that is used to calculate the neutral axis. In other words, the instantaneous neutral axis is supposed to move gradually toward the flange as the load increases and the plate starts to buckle. Since the axial load goes through the original neutral axis, it is equivalent to applying an eccentric load with respect to the instantaneous neutral axis. In other words, without any lateral load, the stiffened panel is expected to buckle toward the flange, i.e., the plate-induced failure mode or flexural buckling. Since the plate buckling occurs prior to the overall panel buckling, one should expect the final failure mode to be a combined plate buckling and column-like flexural buckling in which the stiffener bends toward the flange.

With the presence of the lateral load, the behaviour may be different depending on the direction and magnitude of the lateral load. If the lateral load is applied toward the flange, one should expect a similar deformed shape, i.e. the panel bends toward the flange. On the other hand, if the direction of the lateral load is applied toward the plate but the lateral load is small, the panel can still bend against the lateral load and deform toward the flange. However, if the lateral load is large, the panel will be forced to bend in the opposite direction, i.e. away from the flange. The panel will eventually fail in a mode in which the stiffener twists and bends away from the flange, i.e. a tripping mode.

4.3 Finite element and test results

Specimen 1.2 had no lateral load. As expected, the plate buckled first in an alternate fashion before the peak load. This was then followed by the overall buckling of the panel toward the flange (the plate-induced failure mode). The final deformed shape of the specimen showed a clear picture of the combined plate and overall flexural buckling. As shown in **Figure 13**, the deformed shape of the finite element model is similar to the test observation. The comparison of load-shortening curves is shown in **Figure 14**.

Specimens 1.1 and 1.3 had 10 kN and 25 kN lateral loads, respectively. These lateral loads caused initial compressive stresses in the plate and created initial deflections of 2.4 mm and 6 mm at the mid-span of the stiffener. Since the lateral loads bent the panel toward the flange (in the same direction as the plate-induced failure mode), the final deformed shapes and load-shortening response were also similar to that for specimen 1.2. **Figure 15** shows the deformed shapes at different time steps for specimen 1.1. Step 4 shows the deformation under lateral load, step 13 shows the plate buckling before the peak load, and step 50 shows the final deformed shape. The initial bending deformation had caused the secondary bending moment at mid-span which in turn decreased the peak loads. **Figures**

11

16 and **17** show the final deformed shapes (the finite element model and actual) for specimens 1.1 and 1.3, respectively. **Figures 18** and **19** show the comparison of the load-shortening curves for specimen 1.1 and 1.3, respectively.

Specimens 1.6 and 1.4 were subjected to -10 kN and -25 kN lateral loads, respectively. The test results show both specimens failed in a stiffener-induced failure mode. The stiffener twists and bends toward the plate and transversely. In other words, specimens failed in a tripping mode. **Figure 20** shows the deformed shapes at different time steps for specimen 1.4. Step 4 shows the deformation under lateral load, step 10 shows the deformation before the peak load, and step 50 shows the final deformed shape. The load-shortening curves of specimen 1.4 in **Figure 21** show a steep drop after reaching peak loads for both test and analysis. **Figure 22** shows the final deformed shapes of the finite element model and the specimen 1.4. The finite element model, however, showed completely different behaviour for specimen 1.6. Under -10 kN lateral load, the specimen bent against the lateral load and failed in the plate-induced failure mode as shown in **Figure 23**. Since the deformation is against the lateral load, it requires a larger axial load. As a result, the peak load is 1868 kN which is greater than the peak load of specimen 1.2 (without the lateral load). The results indicated that there is a lateral load at which the model deformation changes from the tripping mode (-25 kN) to the flexural buckling mode (-10 kN).

The lateral load was increased slightly to -15 kN in the second finite element run. This time, the panel failed in the tripping mode and as shown in Figure 24 the peak load dropped suddenly to 1454 kN. The extra 5 kN lateral load only increased the initial lateral deflection at mid-span by 1.2 mm; however, the additional lateral load changed the peak load and the deformed shape dramatically. The average peak load of these two runs is 1661 kN which is very close to the test result of 1673 kN. **Figure 24** shows the load-shortening curves of finite element results and tests.

Specimens 1.7 and 1.5 had 25 kN and -25 kN lateral loads, respectively, but without gripping devices. Both specimens had similar deformed shapes compared to their counterpart specimens 1.3 and 1.4 as shown in **Figures 25** and **26**. The load-shortening curves are shown in **Figures 27** and **28,** respectively. **Table 2** shows the comparisons of specimens with and without edge restraint. The edge restraints did have some effect in changing the peak load.

Table 2: Effect of edge restraint on peak loads

	25 kN lateral load			-25 kN lateral load		
	Specimen	Test	FEA	Specimen	Test	FEA
w/ edge restraint	1.3	1453 kN	1489 kN	1.4	1275 kN	1285 kN
w/o edge restraint	1.7	1361 kN	1436 kN	1.5	1139 kN	1208 kN
	ratio	1.068	1.037	ratio	1.119	1.064

12

5. Discussion

The test of structural components involves heavy machinery including loading and boundary devices. There are some uncertainties associated with these devices. Individually, they may work well but may not move smoothly when assembled together. In addition, the specimen alignment and load application are also associated with some uncertainties. The alignment of the specimen may look perfect to the naked eye, but the contact surface between the specimen and loading head may not be as even as expected. The initial setting of the specimen can change the alignment. These uncertainties can cause some variation in the test results. The finite element models are based on the measured residual stress of a particular specimen and nominal dimensions. The mapping of imperfections to finite element nodal points and the residual stress modelling are an approximation. The residual stresses may change from one specimen to another and the dimension of the specimen may vary from the nominal dimension. In addition, the test specimen is a continuous solid while the finite element idealisation changes a continuous structure to a discrete model. The finite element model based on the displacement formulation is always stiffer than the real structure. Nevertheless, the finite element results have been shown , in most cases, to match the load-shortening response as well as the deformed shapes of the specimens. The differences are small considering the uncertainties associated with the test. The finite element method was proved to be capable of simulating the test procedure.

6. Concluding Remarks

This project demonstrated the capability of the C-FER test frame to test in-plane and laterally loaded stiffened plates. The capability of the finite element method to simulate the test procedure has also been demonstrated. It was found in most cases that the finite element method can produce similar load-shortening response as well as the deformed shape of the specimens.

Both test and analyses have shown the deformed shapes can have either plate-induced or stiffener-induced failure modes depending on the magnitude and direction of the lateral load. The finite element analyses have shown that a slight change in the lateral deflection can result in completely different deformed shapes and dramatically altered peak loads. This indicates the panel is sensitive to geometric imperfection. Criteria in design standards should include a well defined construction tolerance and should consider unexpected lateral loading which may cause a sudden reduction of the peak load.

Finite element results have shown that the magnitude and pattern of residual stress are important and can reduce the peak load. The imperfections, on the other hand, can also influence the peak load as well as the deformed shape. The procedure used to generate the residual stress without altering the imperfection seems to be a reasonable approach.

Five other specimens with the same configuration have been tested. These specimens have

13

deliberately created damage. Since part of the structure became discontinuous, a different mesh arrangement or possible numerical difficulties are expected. These specimens will be analysed in the future.

This project provides important information for improving the buckling and tripping criteria in current design standards. It also gives experimental verification of the simplified numerical models used in predicting overall hull collapse. Because of the successful simulation of the test procedure, panels with other configurations and parameters can be modelled accurately and studied in future. Other types of failure modes such as Grillage and overall hull collapse will also need to be investigated.
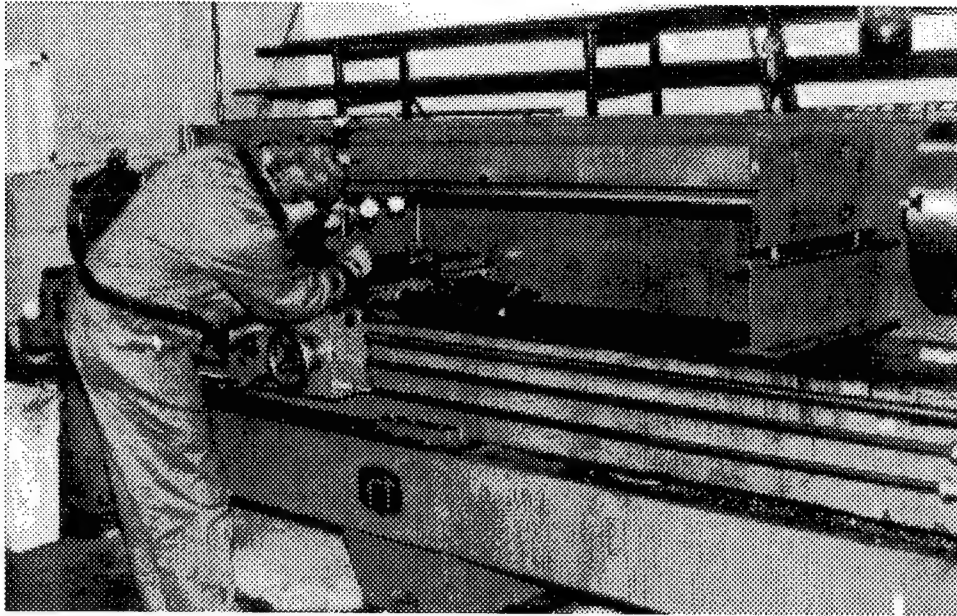
Figure 1: Geometric imperfection measurement
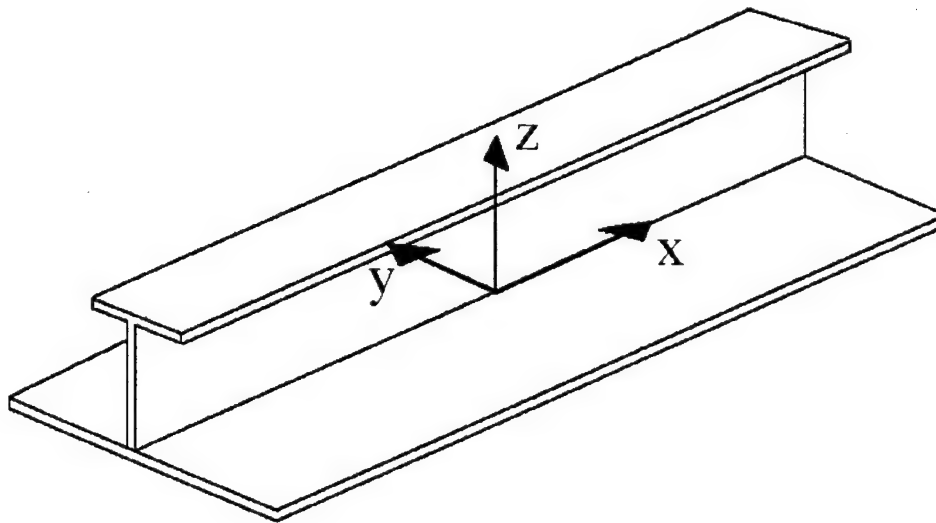
Figure 2: Co-ordinate system
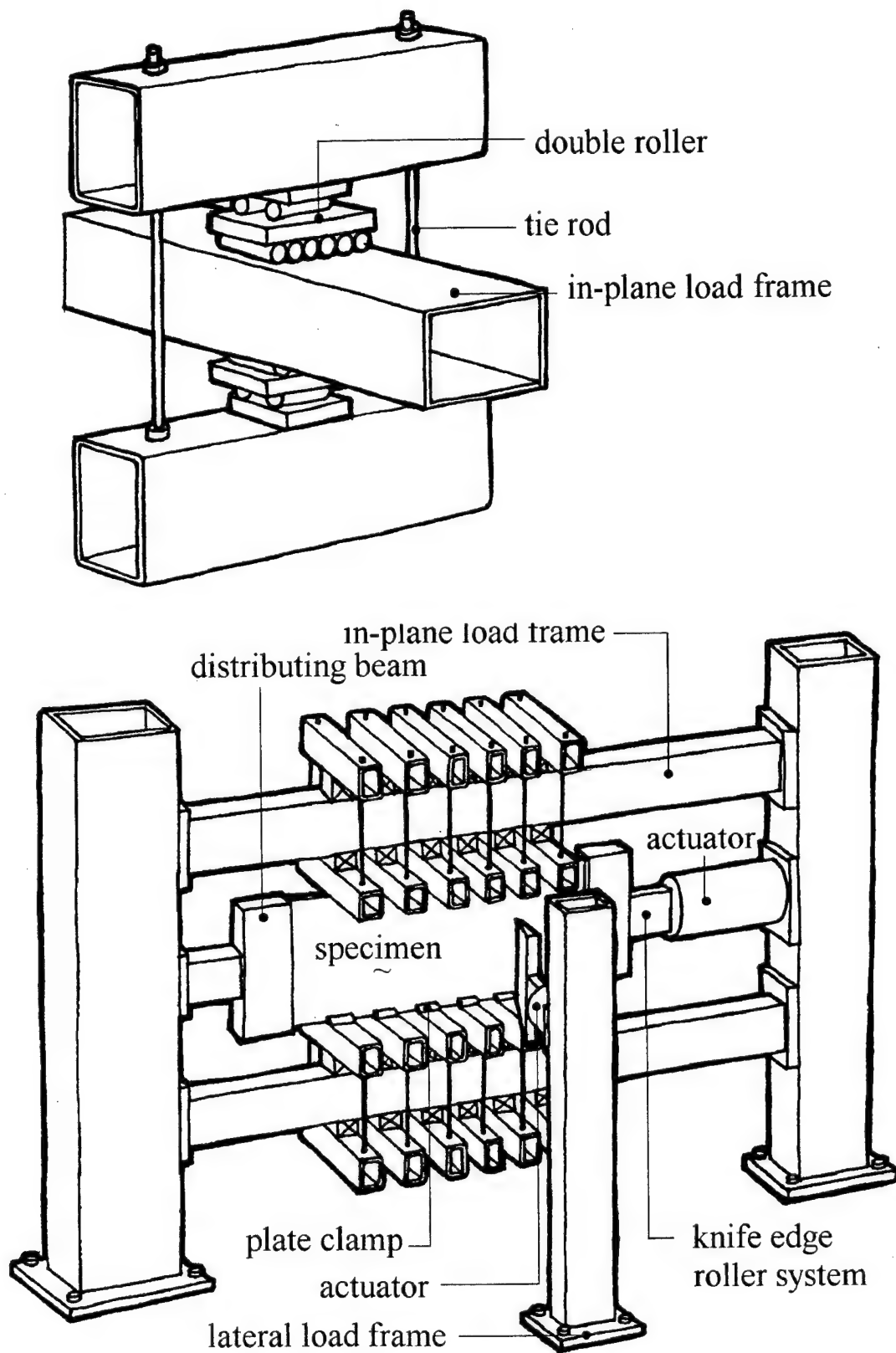
Figure 3: Proposed test set-up
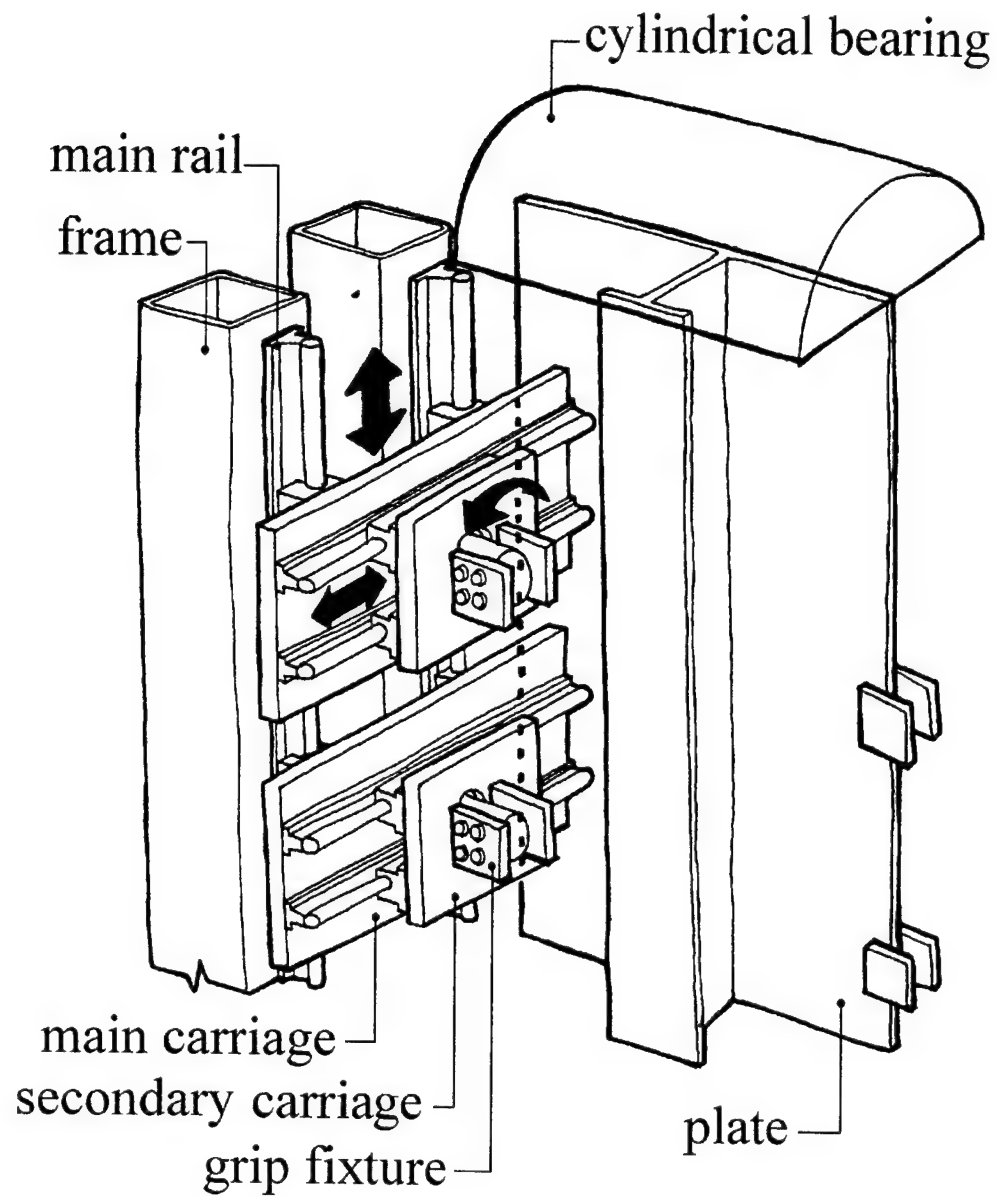
Figure 4: Schematic plot of the final test set-up
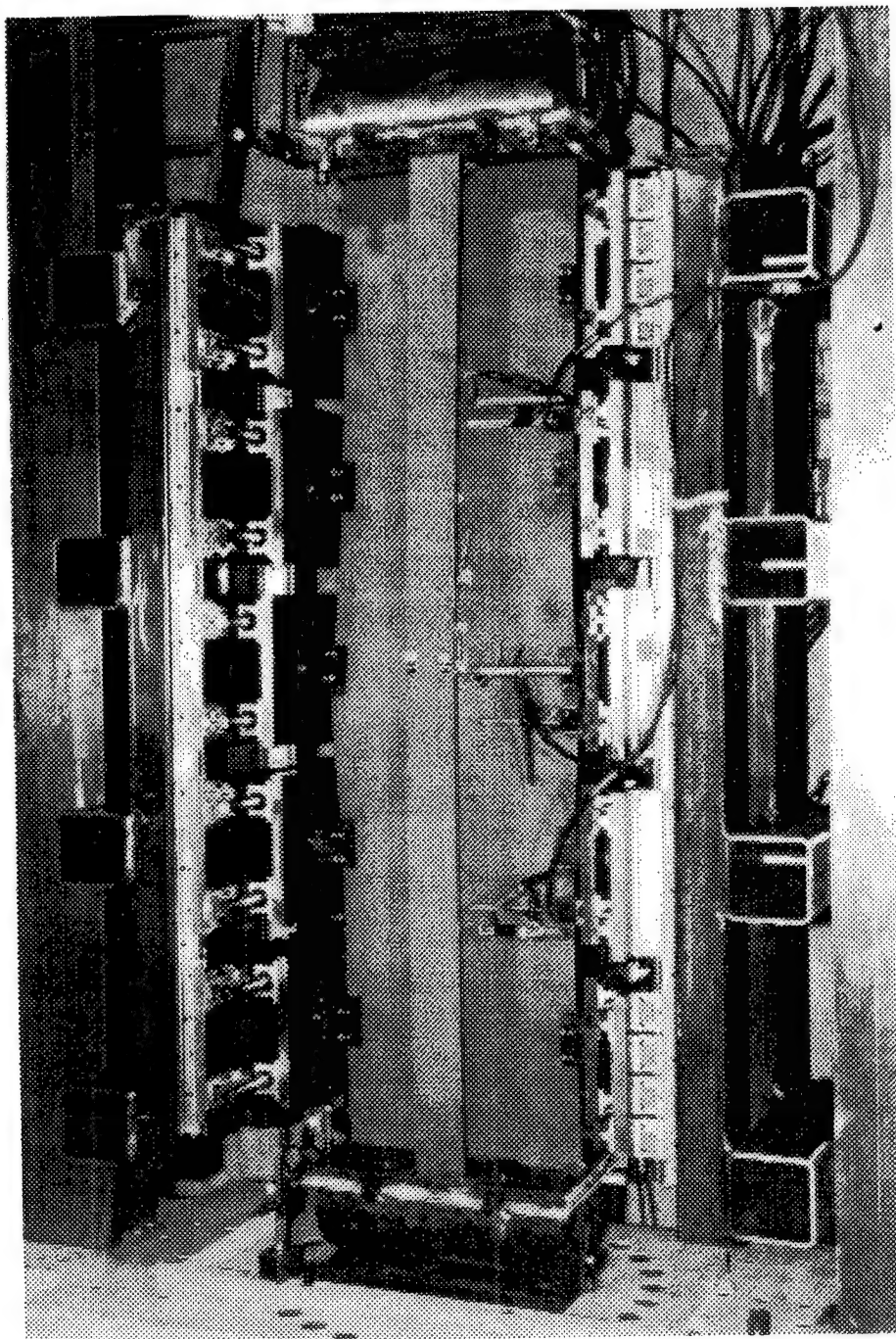
Figure 5: Test set- up
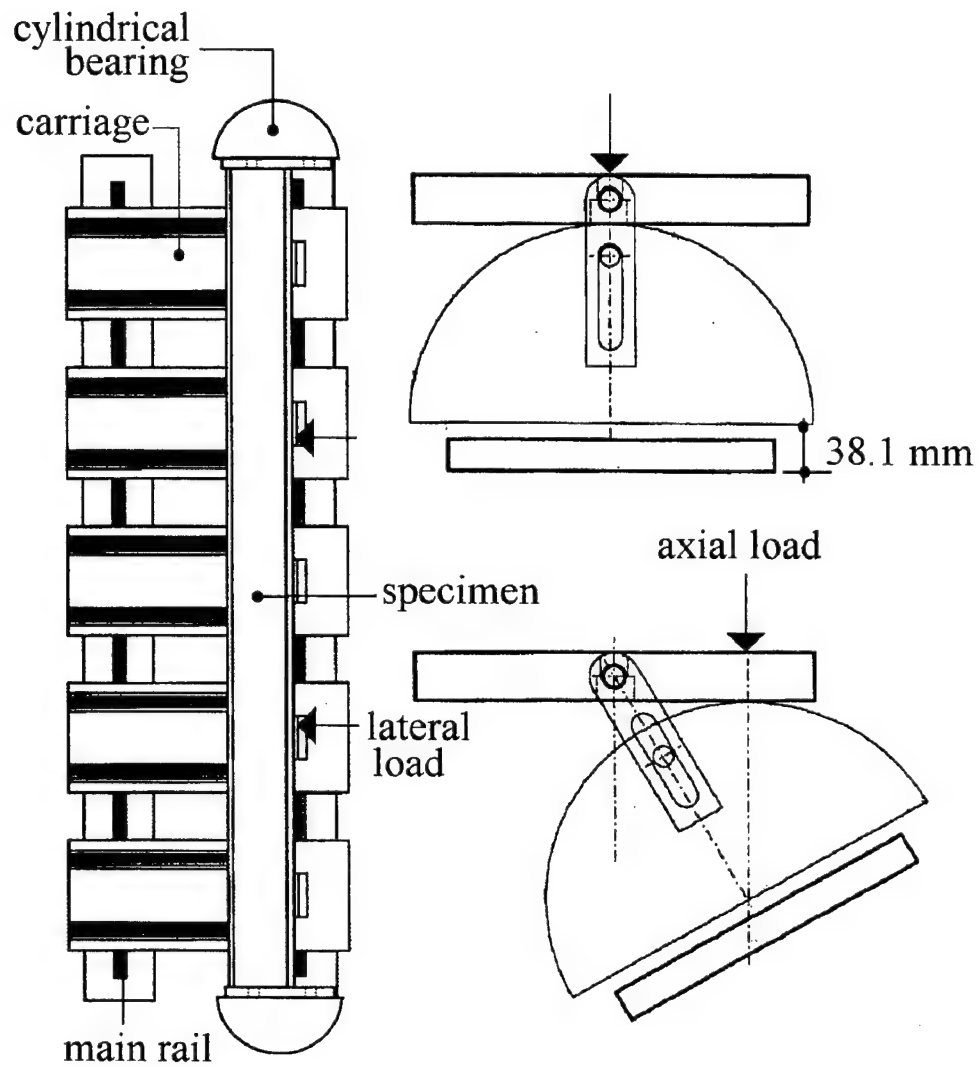
Figure 6: Cross sectional view of the test set-up

test measurement

after extrapolation

finite element mesh
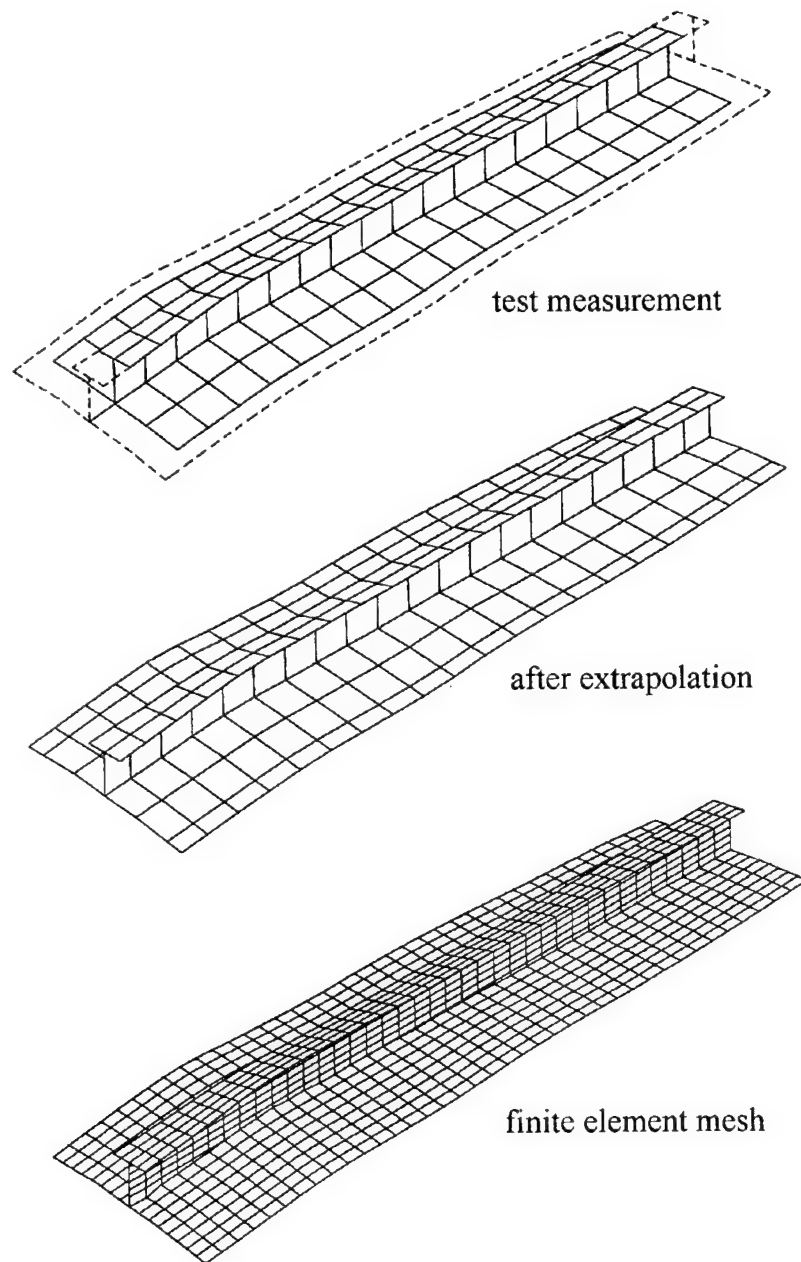
Figure 7: Mapping of the finite element mesh

master node — slave nodes
$U_x, U_y, U_z = 0$

(case 1)

grip
fixture

slave
node

master
node

$R_x, U_y, R_z = 0$

(case 2)
thicker
plate

$R_x, U_y, R_z = 0$

x

y

z

O

slave nodes

master node
$U_y, U_z = 0$
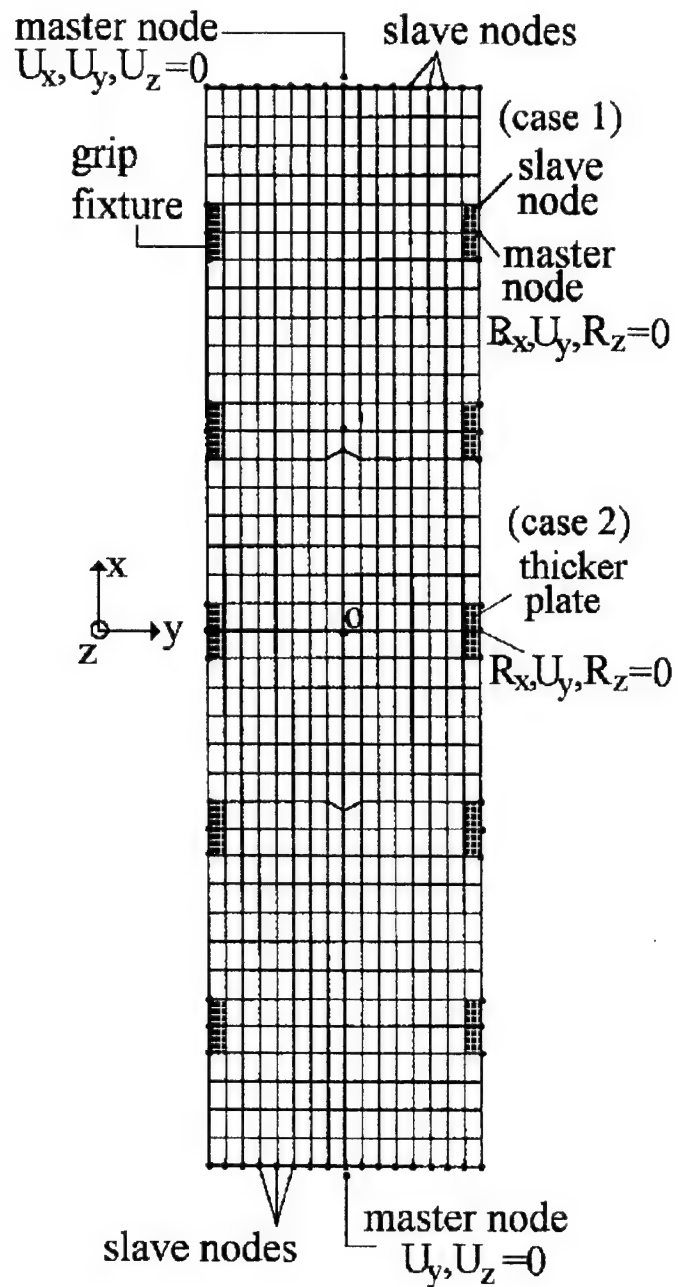
Figure 8: Boundary condition
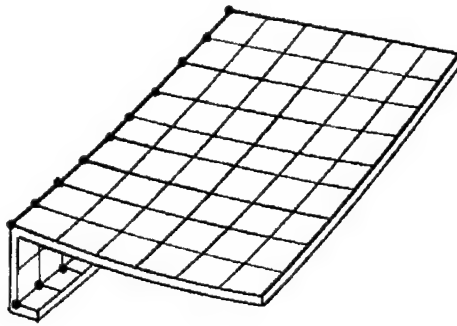
STEP 1
- Map test measurements to F.E. nodal points
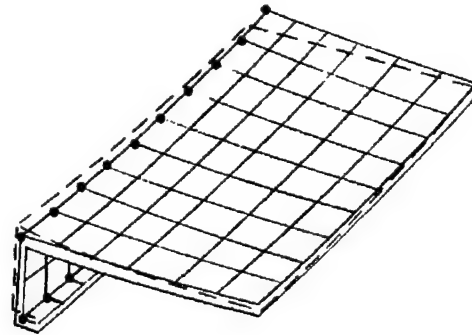
STEP 2
- Increase temperature
- Generate reversed residual stresses
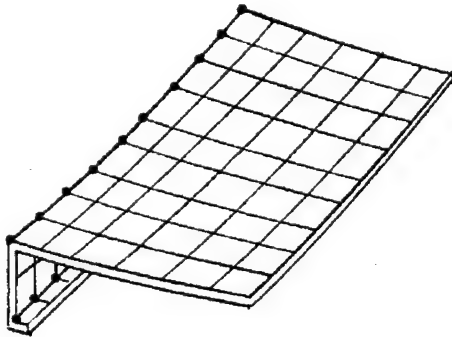
STEP 3
- Current geometry as original geometry w/o residual stresses
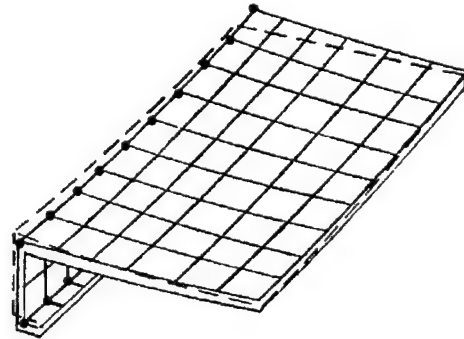
STEP 4
- Decrease temperature
- Produce desired residual stresses and imperfections

Figure 9: Residual stress and imperfection modeling
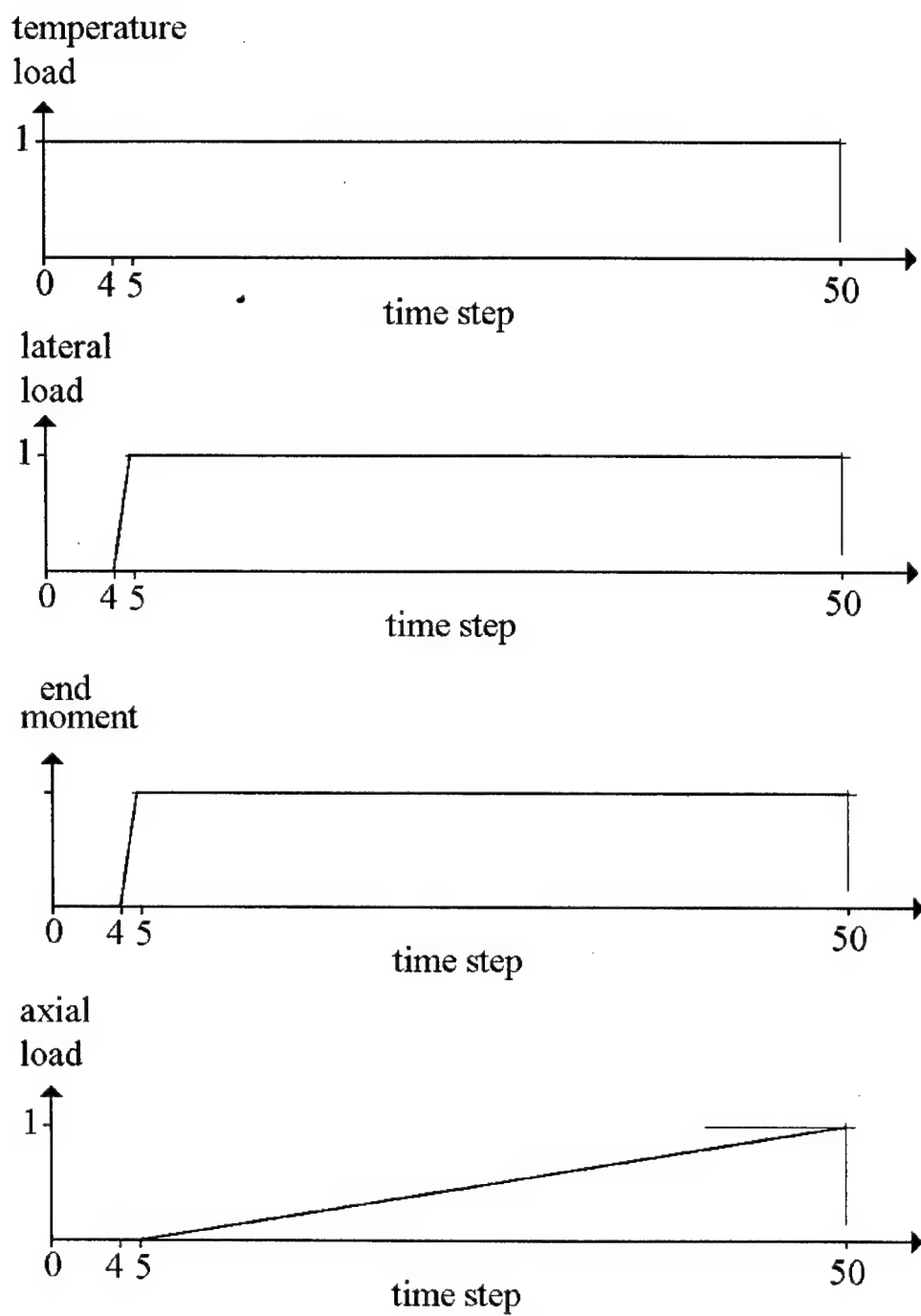
Figure 10: Time function

Residual Stress at Plate
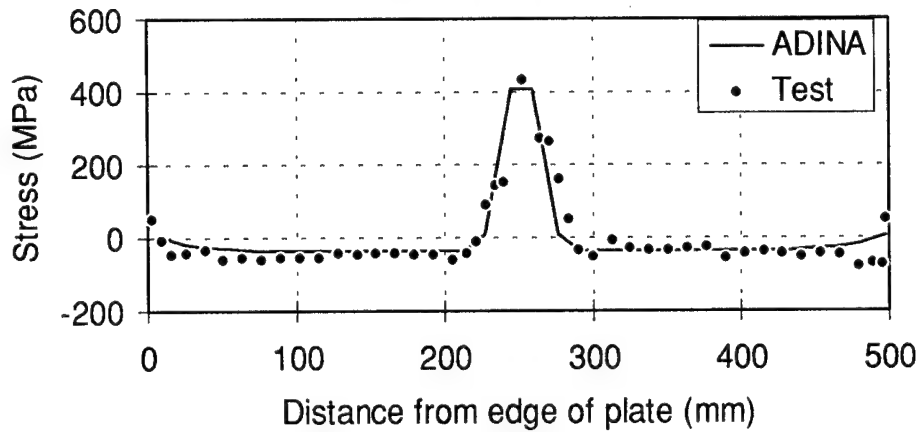
Residual Stress at Flange
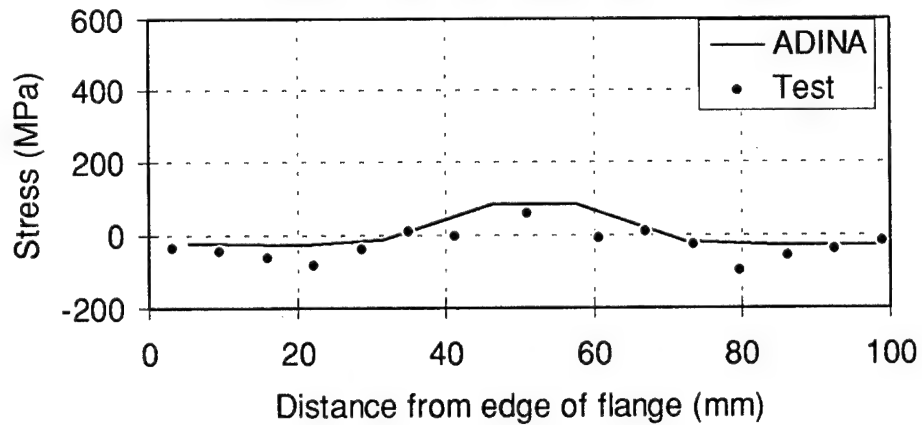
Residual Stress at Web
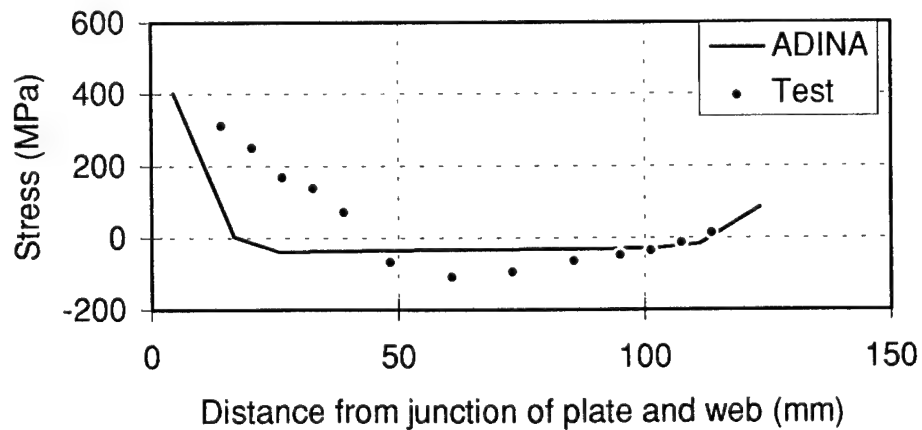
Figure 11: Residual stress patterns

24
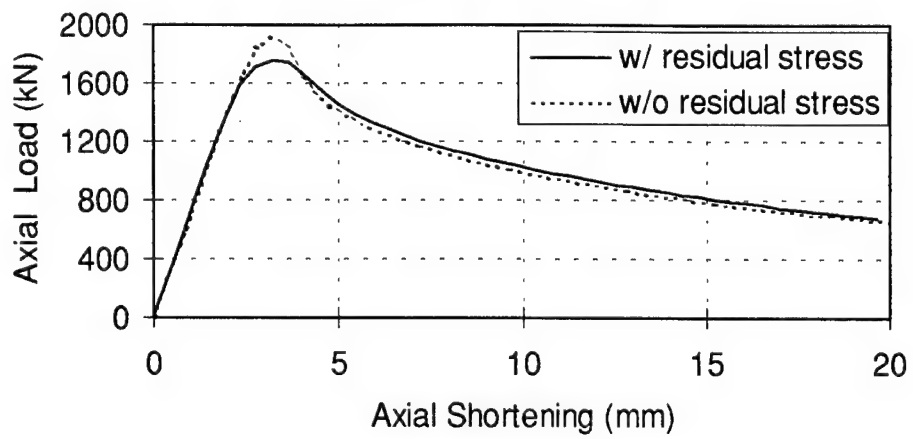
Specimen 1.2

Figure 12: Effect of the residual stress
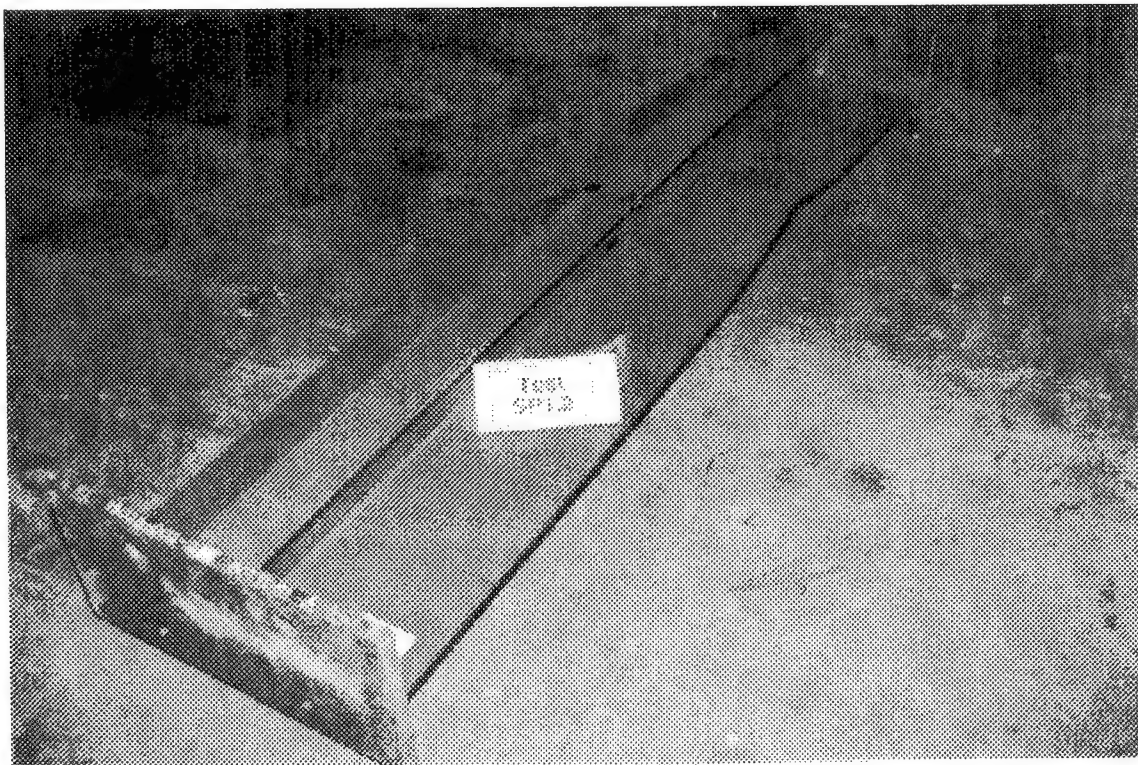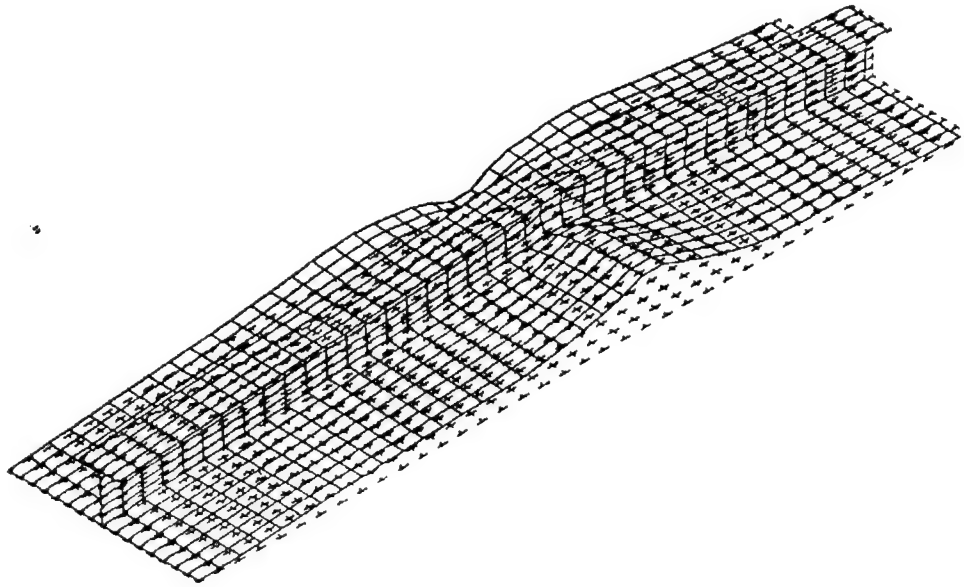
Figure 13: Final deformed shape of specimen 1.2
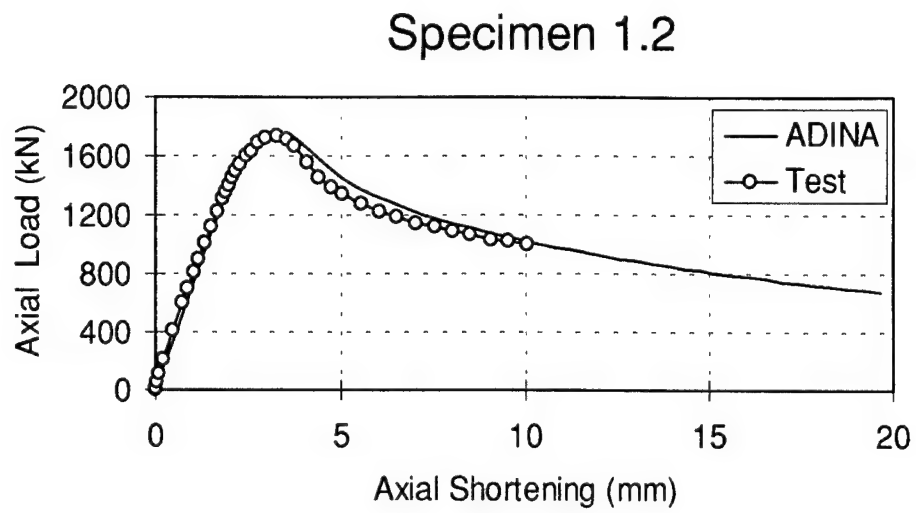
Specimen 1.2

Figure 14: Load-shortening curve of specimen 1.2

step 4

step 13
peak load

step 50
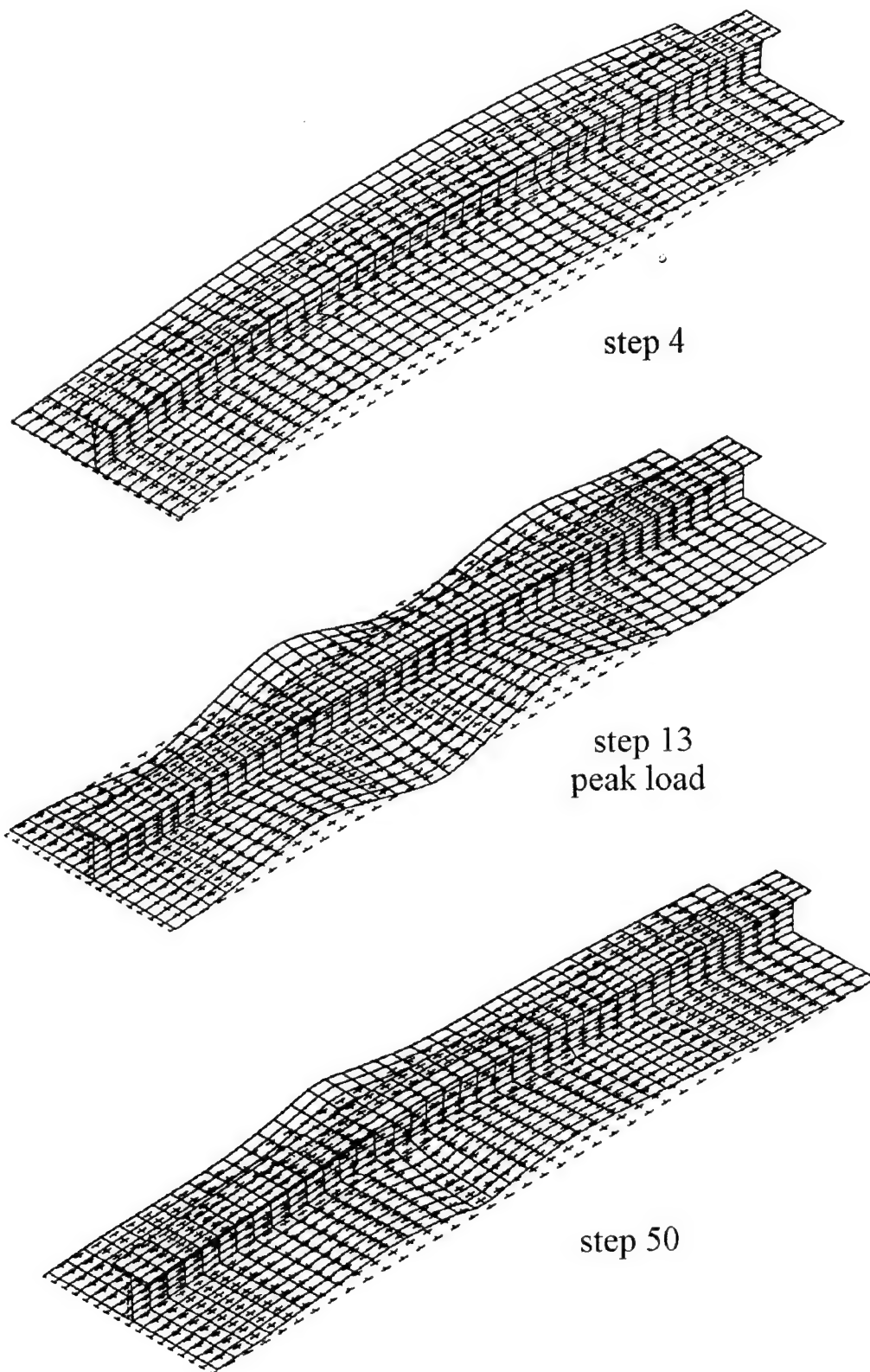
Figure: 15: Deformed shapes of specimen 1.1 at different time steps
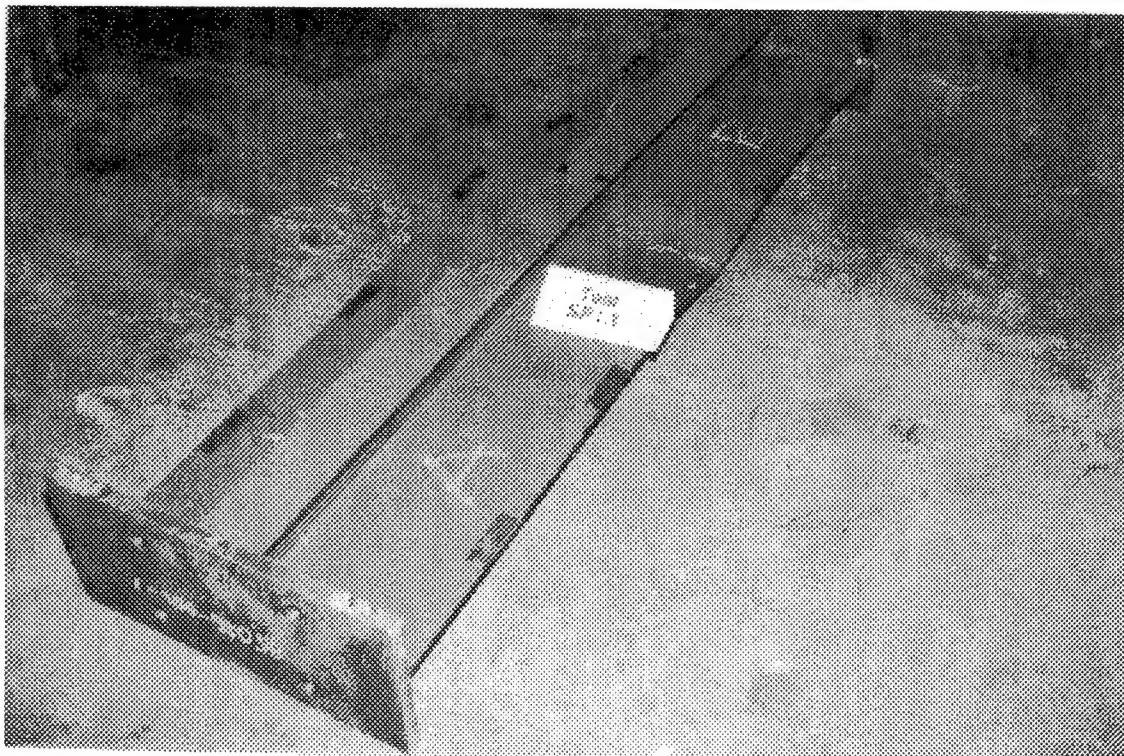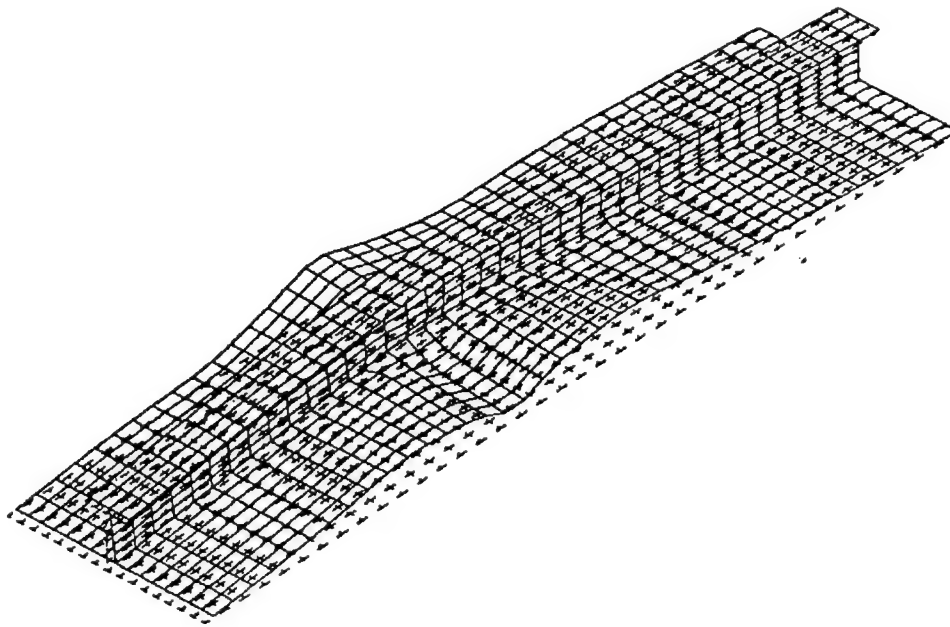
Figure 16: Final deformed shape of specimen 1.1
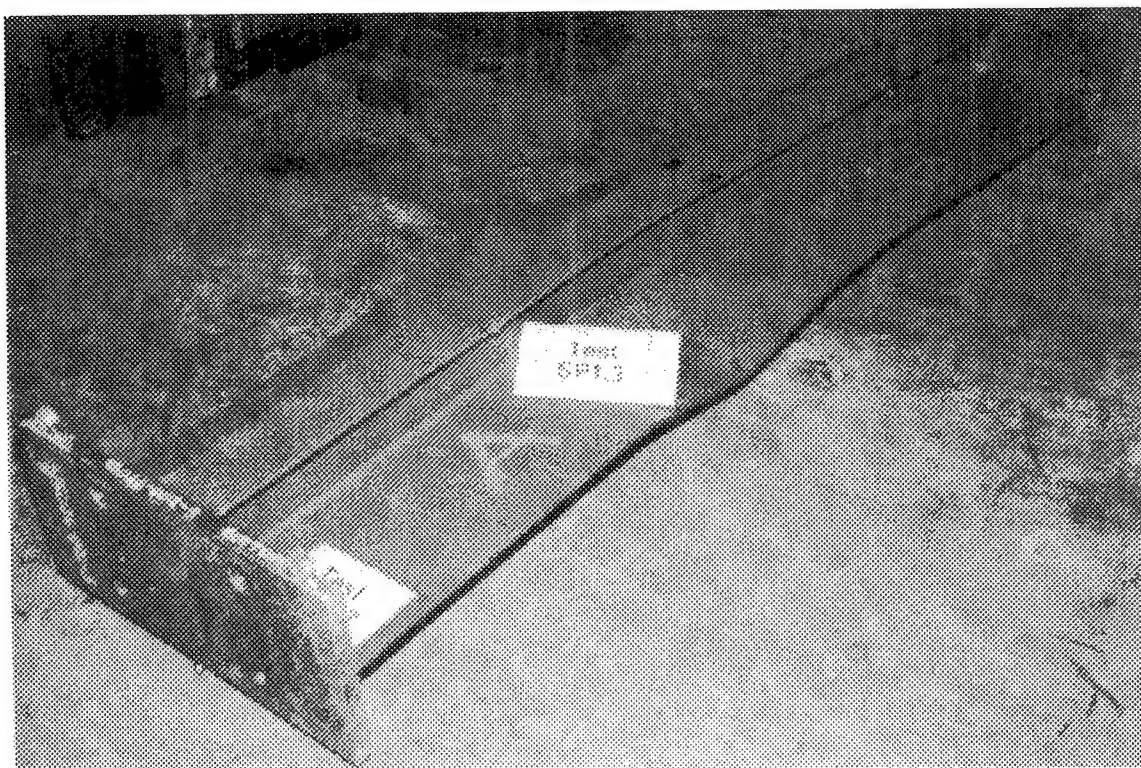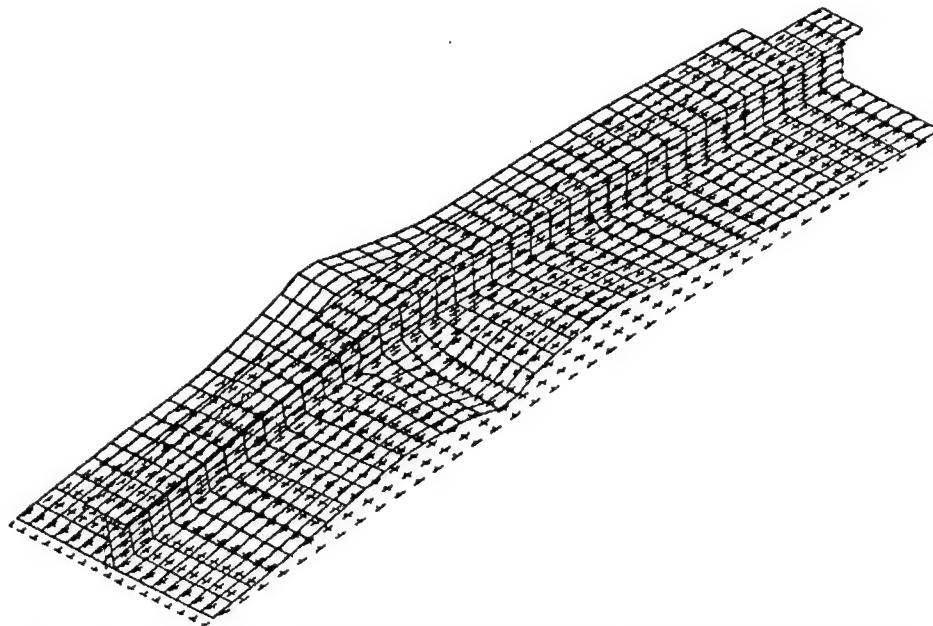
Figure 17: Final deformed shape of specimen 1.3

Specimen 1.1
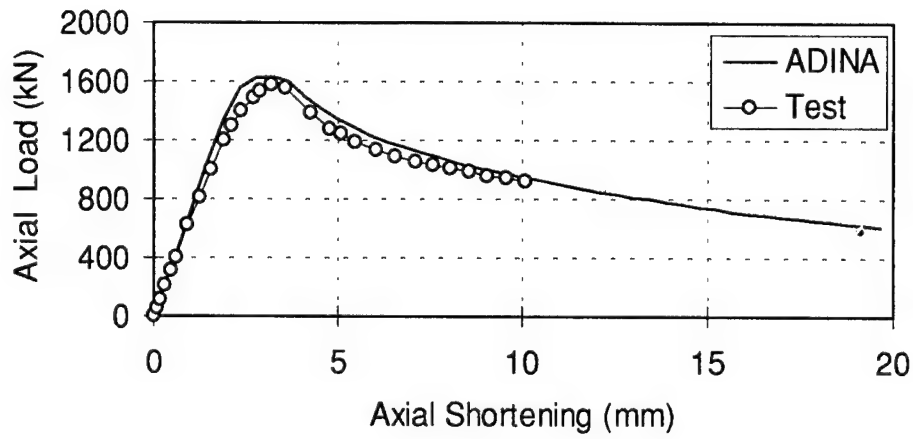
Figure 18: Load-shortening curve of specimen 1.1

Specimen 1.3
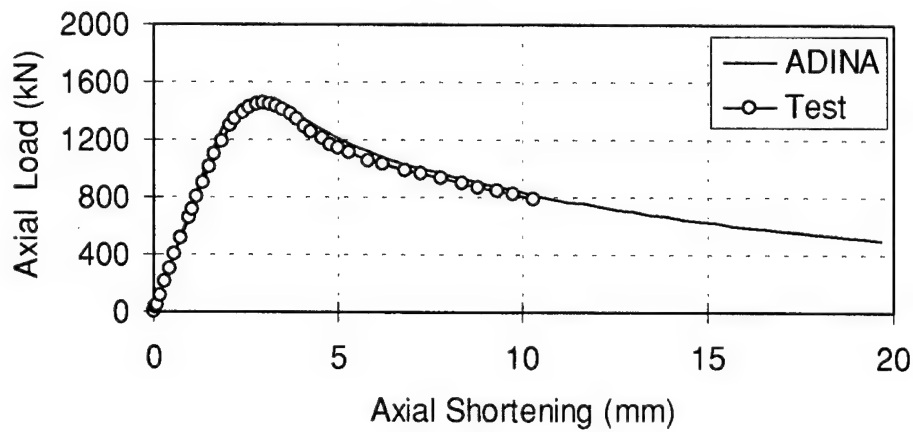
Figure 19: Load-shortening curve of specimen 1.3

step 4

step 10
peak load

step 50
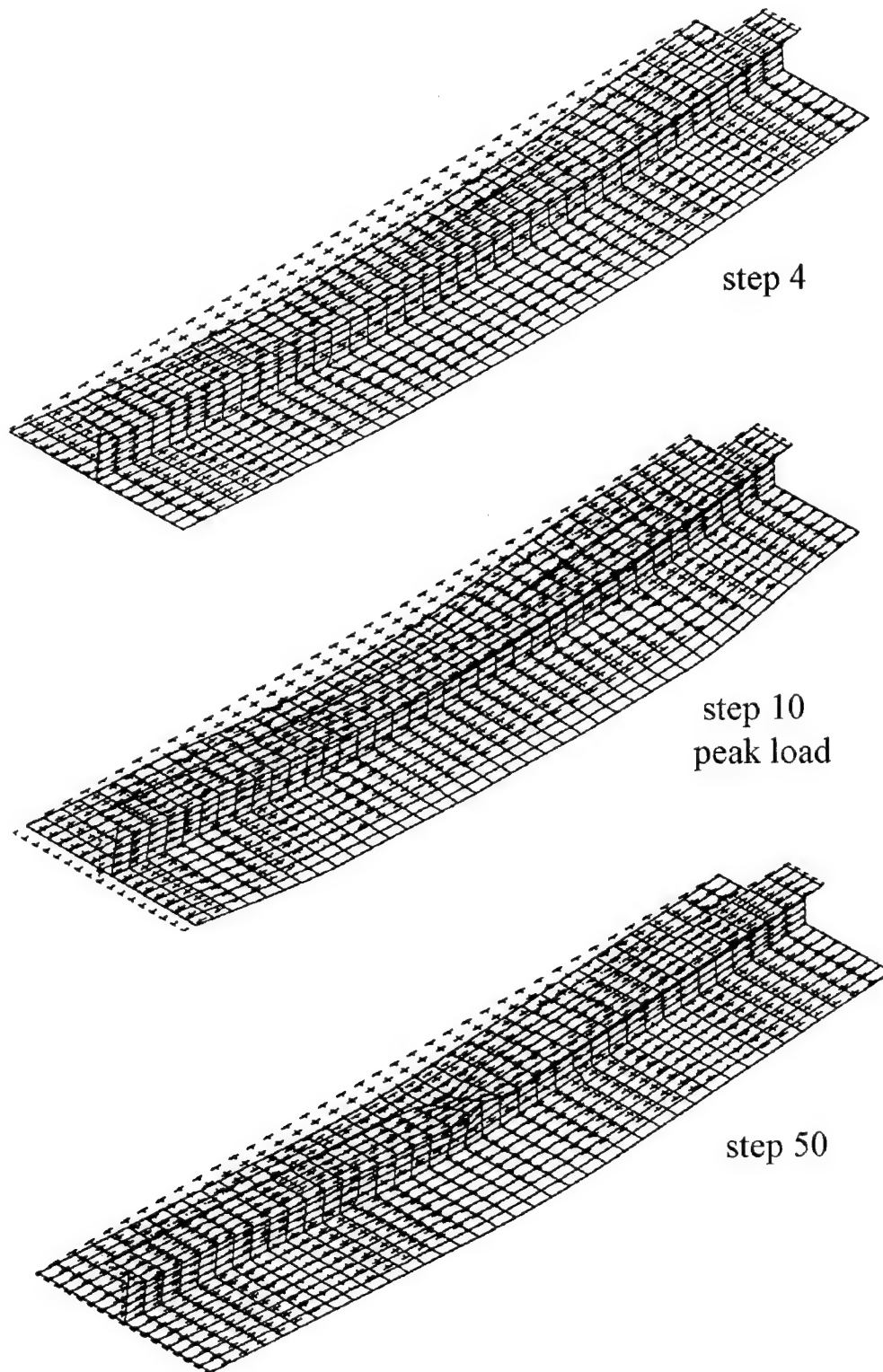
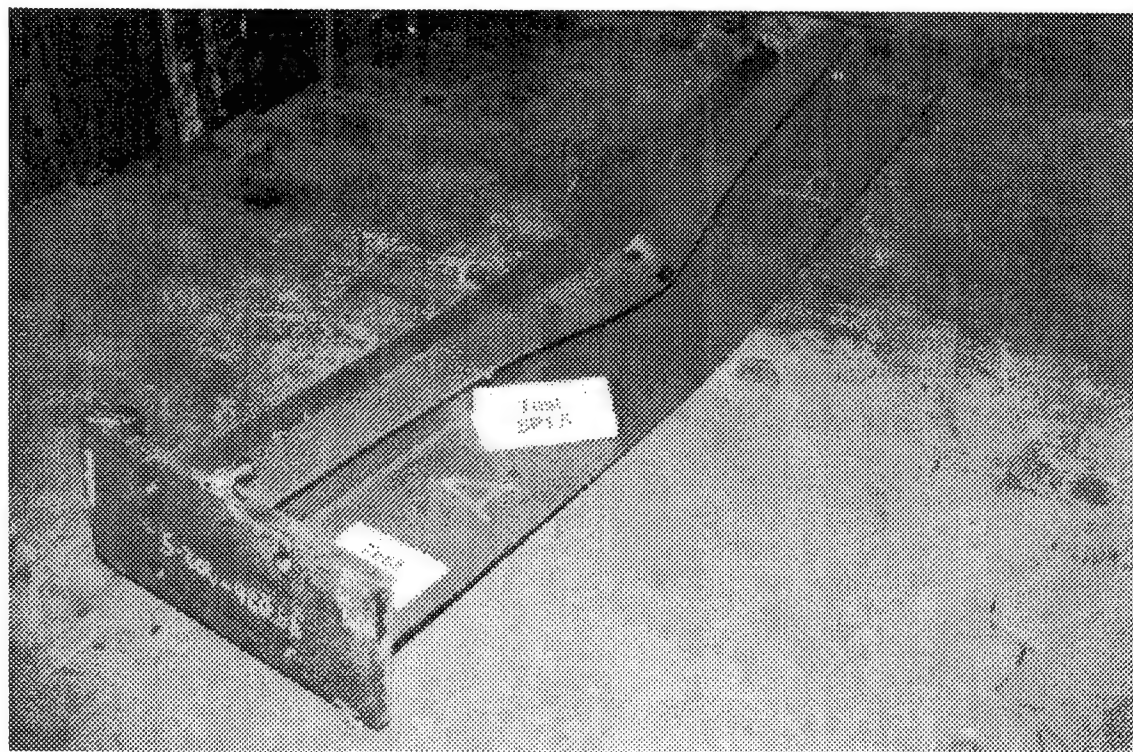**Figure 20: Deformed shapes of specimen 1.4 at different time steps**
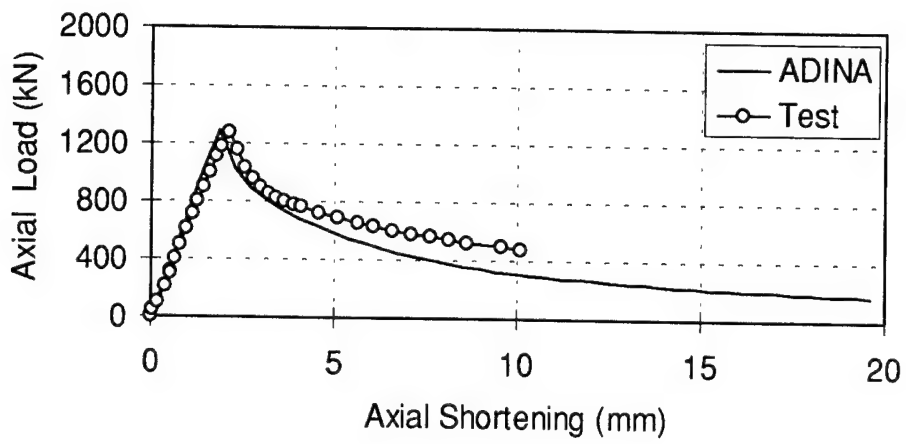
Figure 21: Load-shortening curve of specimen 1.4
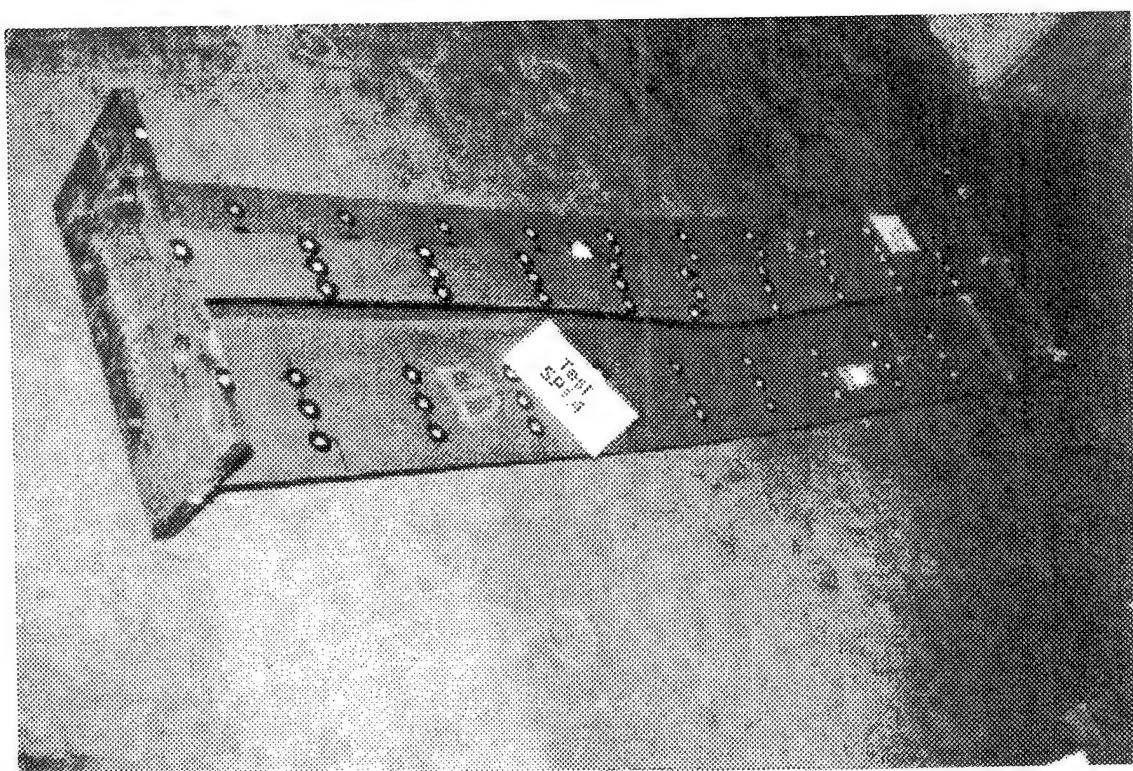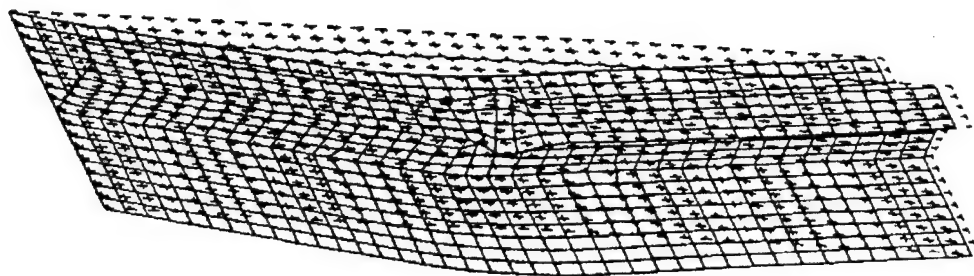
Figure 22: Final deformed shape of specimen 1.4

-10 kN
lateral load

-15 kN
lateral load
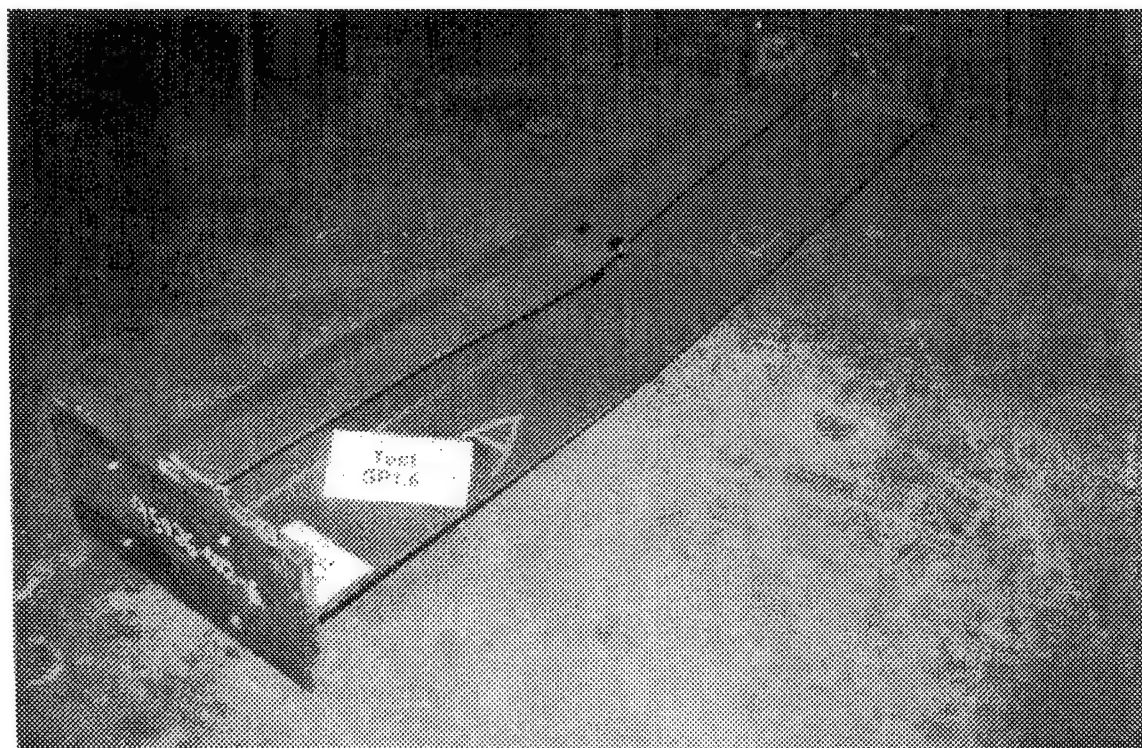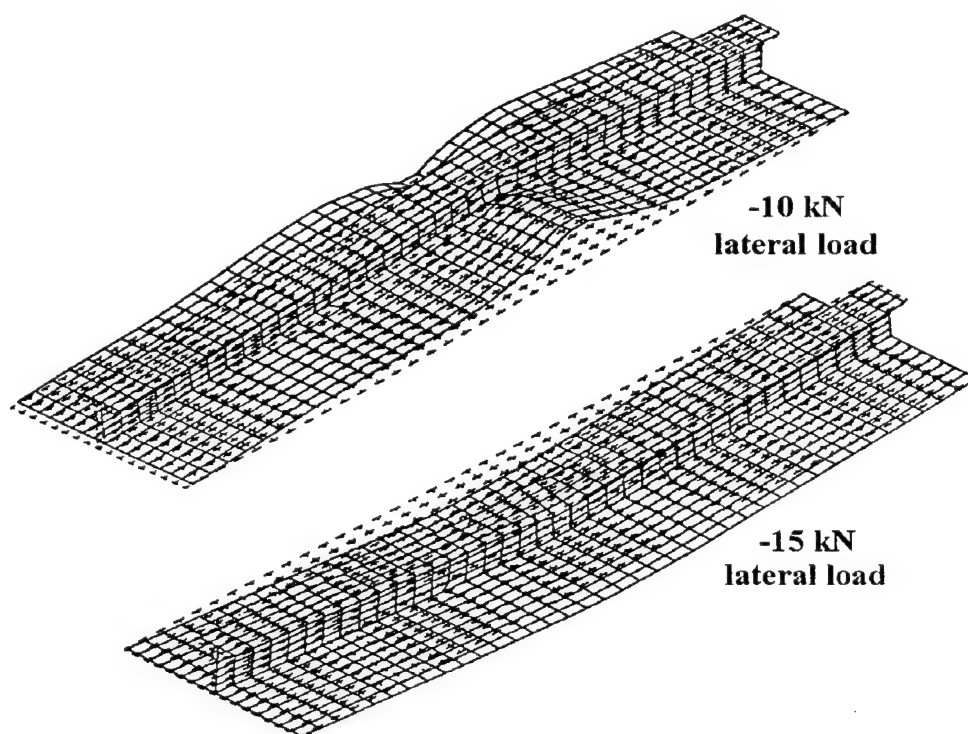
Figure 23: Final deformed shape of specimen 1.6
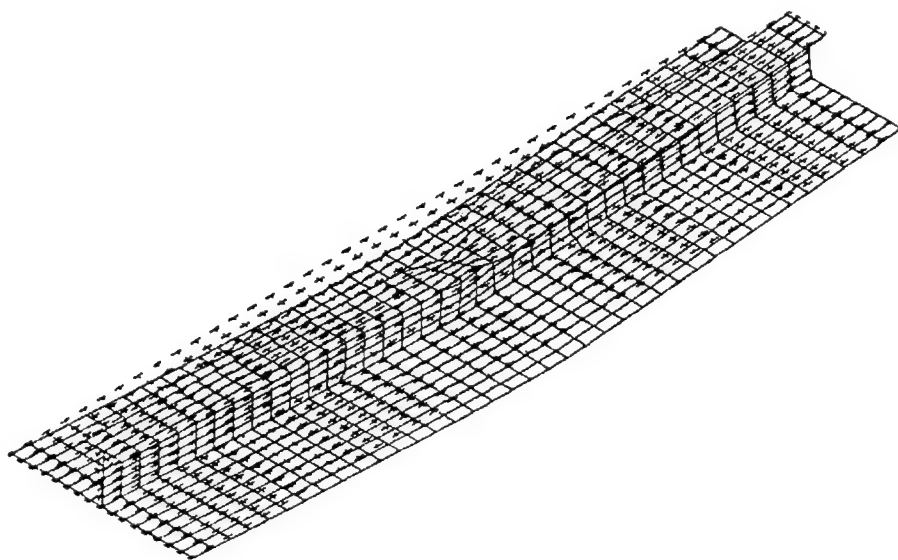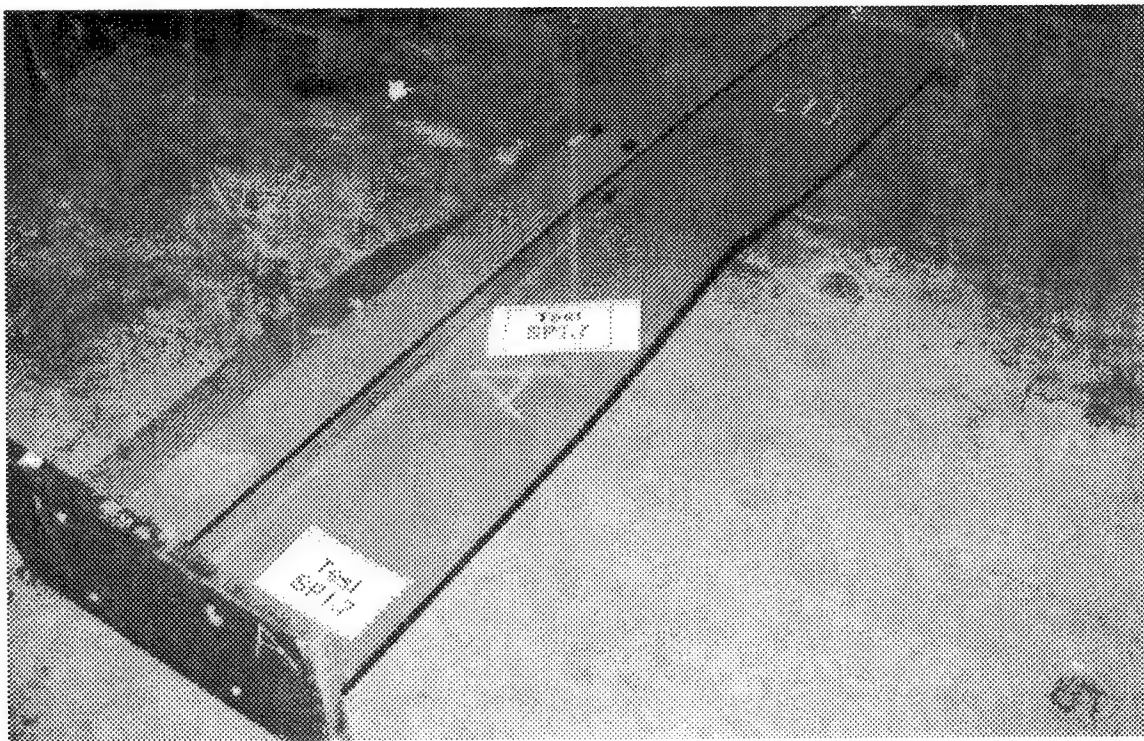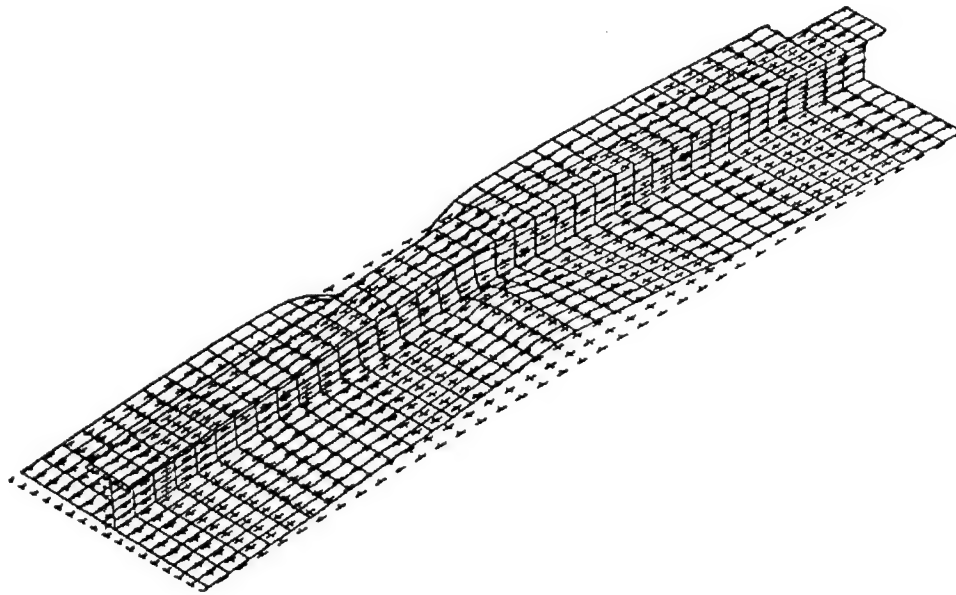
Specimen 1.6
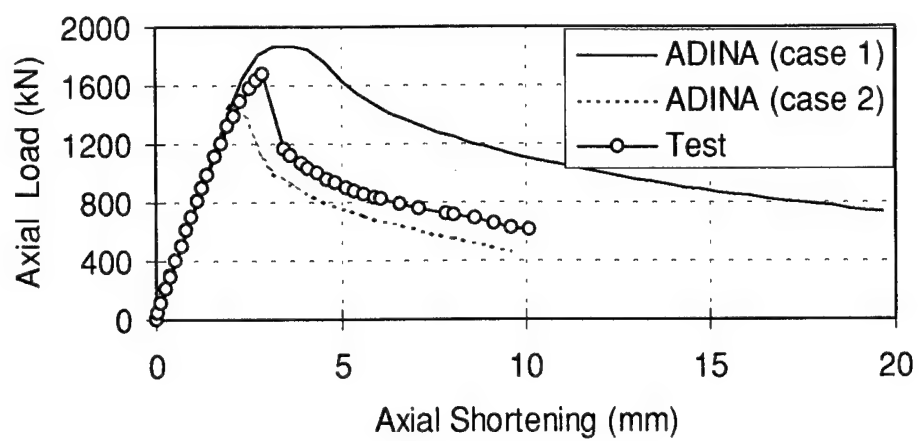
Figure 24: Load-shortening curve of specimen 1.6

Figure 25: Final deformed shape of specimen 1.5

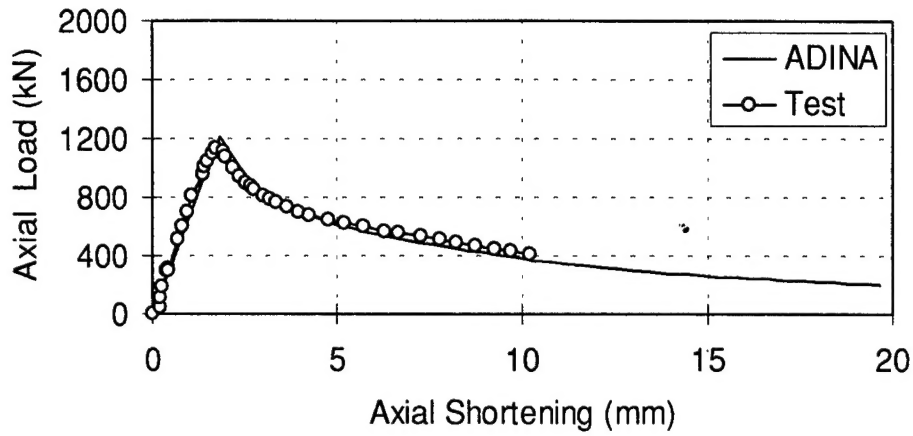**Figure 26: Final deformed shape of specimen 1.7**

Specimen 1.5

Figure 27: Load-shortening curve of specimen 1.5
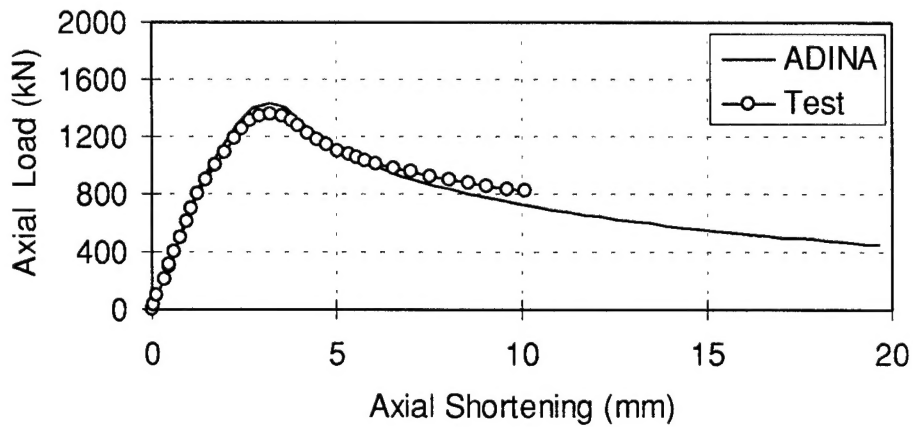
Specimen 1.7

Figure 28: Load-shortening curve of specimen 1.7

6. References

1. "Standard for the Structural Design of Canadian Forces Surface Ships", D-03-002-008/SG-002, DSE 5-4, Department of National Defence, 1993.

2. Hu., S.Z., "A Numerical Study of Tripping Behaviour of Stiffened Plates", Proc. 2nd Canadian Marine Dynamics Conference, pp. 203-210, 1993.

3. "Guidelines on Design and Analysis of Steel Structures in the Petroleum Activity", Norwegian Petroleum Directorate, 1990.

4. Hu, S.Z., "EBMS - A Program for Equivalent Beam Modelling of Ship Structure", DREA Technical Memorandum 95/208, April 1995.

5. Dow, R.S. and Smith, C.S., "FABSTRAN: A Computer Program for FRame and Beam Static and Transient Response Analysis", Admiralty Research Establishment, ARE TR 86205, Dec. 1986

6. "ADINA-IN for ADINA Users Manual", Report ARD 90-4, ADINA R & D, Inc., Sept. 1990.

7. Hu, S.Z., "An Analytical Investigation of the Compressive Behaviour of Fabricated Steel Tubes", Ph.D. Dissertation, Dept. of Civil Engineering, University of Toronto, 1991.

8. Hu, S.Z., "A Finite Element Assessment of the Buckling Strength Equations of Stiffened Plates", Proc. Ship Structures Symposium '93, pp. J1-J10, 1993.

DOCUMENT CONTROL DATA

(Security classification of title, body of abstract and indexing annotation must be entered when the overall document is classified)

1. ORIGINATOR (The name and address of the organization preparing the document. Organizations for whom the document was prepared, e.g. Establishment sponsoring a contractor's report, or tasking agency, are entered in section 8.)	2. SECURITY CLASSIFICATION (Overall security of the document including special warning terms if applicable.)
Defence Research Establishment Atlantic P.O. Box 1012, Dartmouth, N.S. B2Y 3Z7	UNCLASSIFIED

3. TITLE (The complete document title as indicated on the title page. Its classification should be indicated by the appropriate abbreviation (S,C,R or U) in parentheses after the title.)

Nonlinear Finite Element Simulation of the Test Proceedure for Stiffened Panels under Combined Lateral and In-plane Loads

4. AUTHORS (Last name, first name, middle initial. If military, show rank, e.g. Doe, Maj. John E.)

HU, Thomas S.Z.

5. DATE OF PUBLICATION (Month and year of publication of document.) March1997	6a. NO. OF PAGES (Total containing information. Include Annexes, Appendices, etc.) 45	6b. NO. OF REFS. (Total cited in document.) 8

6. DESCRIPTIVE NOTES (The category of the document, e.g. technical report, technical note or memorandum. If appropriate, enter the type of report, e.g. interim, progress, summary, annual or final. Give the inclusive dates when a specific reporting period is covered.)

DREA Technical Memorandum

8. SPONSORING ACTIVITY (The name of the department project office or laboratory sponsoring the reseach and development. include the address.)

Defence Research Establishment Atlantic
P.O. Box 1012, Dartmouth, N.S.   B2Y 3Z7

9a. PROJECT OR GRANT NUMBER (If appropriate, the applicable research and development project or grant number under which the document was written. Please specify whether project or grant.) 1.g.c.	9b. CONTRACT NUMBER (If appropriate, the applicable number under which the document was written.)

10a. ORIGINATOR'S DOCUMENT NUMBER (The official document number by which the document is identified by the originating activity. This number mrst be unique to this document.) DREA Technical Memorandum 97/219	10b. OTHER DOCUMENT NUMBERS (Any other numbers which may be assigned this document either by the originator or by the sponsor.)

11. DOCUMENT AVAILABILITY (Any limitations on further dissemination of the document, other than those imposed by security classification)

(X) Unlimited distribution
(   ) Distribution limited to defence departments and defence contractors; further distribution only as approved
(   ) Distribution limited to defence departments and Canadian defence contractors; further distribution only as approved
(   ) Distribution limited to government departments and agencies; futher distribution only as approved
(   ) Distribution limited to defence departments; further distribution only as approved
(   ) Other (please specify):

12. DOCUMENT ANNOUNCEMENT (Any limitation to the bibliographic annoucement of this document. This will normally correspond to the Document Availability (11). However, where futher distribution (beyond the audience specified in 11) is possible, a wider announcement audience may be selected.)

DCDO3 2/06/87

13. ABSTRACT (a brief and factual summary of the document. It may also appear elsewhere in the body of the document itself. It is highly desirable that the abstract of classified documents be unclassified. Each paragraph of the abstract shall begin with an indication of the security classification of the information in the paragraph (unless the document itself is unclassified) represented as (S), (C), (R), or (U). It is not necessary to include here abstracts in both official languages unless the text is bilingual).

DREA conducted a joint structural testing project with the U.S. Interagency Ship Structures Committee (SSC) at C-FER (Centre For Engineering Research Inc., Edmonton) earlier this year. Twelve stiffened plates, seven without damage and five with damage, having dimensions approximately equal to a typical stiffened panel at the strength deck of the Canadian Patrol Frigate (CPF) were tested. One of the objectives of this project was to conduct a computer simulation of the test procedure with the non-linear finite element method. It was hoped that after a successful simulation, panels with other dimensions and parameters could be studied numerically. As the scientific authority of this project, the author planned the test procedure, conducted the numerical prediction of the collapse load of the specimens, and performed the computer simulation of the test procedure. Because of the complexity of the computer simulation and completely different behaviour between damaged and undamaged specimens, this memorandum only summarises the finite element results on specimens without damage and their relation with the test observations. Seven specimens, which failed either in tripping or in combined plate and flexural buckling modes under combined lateral and axial loads, were modelled. Some interesting buckling phenomena were discovered and are discussed.

14. KEYWORDS, DESCRIPTORS or IDENTIFIERS (technically meaningful terms or short phrases that characterize a document and could be helpful in cataloguing the document. They should be selected so that no security classification is required. Identifiers, such as equipment model designation, trade name, military project code name, geographic location may also be included. If possible keywords should be selected from a published thesaurus. e.g. Thesaurus of Engineering and Scientific Terms (TEST) and that thesaurus-identified. If it not possible to select indexing terms which are Unclassified, the classification of each should be indicated as with the title).

Stiffened Panel

Non-linear Finite Element Method

Test Set-up

Residual Stress

Initial Imperfections